UNCERTAINTY OF PHOSPHORUS LOADINGS ESTIMATION USING VOLLENWEIDER MODEL FOR RESERVOIR EUTROPHICATION CONTROL

(KETAKPASTIAN BEBANAN FOSFORUS MENGGUNAKAN MODEL VOLLENWEIDER UNTUK KAWALAN EUTROFIKASI TAKUNGAN)

SUPIAH SHAMSUDIN
SOBRI HARUN
AZMI AB RAHMAN

PUSAT PENGURUSAN PENYELIDIKAN
UNIVERSITI TEKNOLOGI MALAYSIA

2009

UNCERTAINTY OF PHOSPHORUS LOADINGS ESTIMATION USING VOLLENWEIDER MODEL FOR RESERVOIR EUTROPHICATION CONTROL

(KETAKPASTIAN BEBANAN FOSFORUS MENGGUNAKAN MODEL VOLLENWEIDER UNTUK KAWALAN EUTROFIKASI TAKUNGAN)

SUPIAH SHAMSUDIN
SOBRI HARUN
AZMI AB RAHMAN

RESEARCH VOTE NO:
78138

Jabatan Hidraul dan Hidrologi
Fakulti Kejuruteraan Awam
Universiti Teknologi Malaysia

2009

UNCERTAINTY OF PHOSPHORUS LOADINGS ESTIMATION USING VOLLENWEIDER MODEL FOR RESERVOIR EUTROPHICATION CONTROL

Keywords : Phosphorus, Loadings, Uncertainty, Vollenweider, Reservoir, Eutrophocatin

Eutrophication process downgraded lake or reservoir water quality, if the system is not monitored and managed properly. Recent investigation seems to favor phosphorus as the limiting factor for reservoir productivity. The purpose of this study is to estimate the uncertainty of phosphorus loadings for the Layang reservoir using Vollenweider-IHACRES model. The incorporation of IHACRES Model had helped to compute better hydrological estimation. This model is used to predict the streamflow into the reservoirs that later be used in the Vollenweider model. Rainfall data were obtained from the Department of Irrigation and Drainage Malaysia for the Station 1539001, Loji air Sungai Layang. Five water samples were taken randomly near the inlet and upstream of reservoir. The water samples were tested with reagent phos Ver 3 phosphate using DR 4000 (Hach Co. CO 80539-9987, USA) to indicate the dissolved phosphorus content in mg/l. The total phosphorus concentration obtained from the three site visits were observed. The average phosphorus content was 0.214 mg/l. The highest phosphorus content observed was 0.622 mg/l and the lowest concentration was 0.053 mg/l. Fuzzy membership function is then used to describe phosphorus content, hydraulic loadings and the phosphorus loadings that represent the current conditions of the reservoir. By using fuzzy membership function, a range of estimation could be obtained. The most likely range of phosphorus content obtained was 0.1 mg/l to 0.3 mg/l and for hydraulic loadings was 1350 m/yr to 1400 m/yr. Estimated phosphorus loadings range from 0.26 $g/m^2/yr$ to 0.81 $g/m^2/yr$ (7.81 ton/yr to 24.28 ton/yr). The average phosphorus content was 0.214 mg/l and average hydraulic loading was 1452.25 m/yr. The average phosphorus loading calculated was 0.6$g/m^2/yr$, within the estimated range of 0.26$g/m^2/yr$ to 0.81$g/m^2/yr$. The largest bias from the IHACRES model simulation is -0.5546 mm/day and the smallest bias is -0.0076 mm/day. The highest R^2 value is 0.9925 while the lowest is 0.9208. Both statistics showed that the model is able to perform well. This fuzzy phosphorus loadings estimation will help lake water quality improvement and management in the future. In order to ensure the phosphorus level reduction and overall lake water quality, the development and overall activities within the watershed should be properly and systematically managed.

Key researchers :

Assoc Prof Dr Supiah Shamsudin
Assoc Prof Dr Sobri Harun
Assoc Prof Dr Azmi Ab Rahman

Email : supiah@utm.my, supiahsham@yahoo.com
Tel No. : 607-5531581
Vot No. : 78138

ABSTRAK

Eutrofikasi akan memburukkan sesebuah tasik atau reservor jika sistem ini tidak dipantau dan diuruskan dengan baik. Kajian terkini lebih condong dan yakin fosforus adalah faktor pengehad untuk pengeluaran tasik. Tujuan kajian ini adalah untuk menganggar ketakpastian bebanan fosforus kedalam Reservor Layang dengan menggunakan model Vollenweider-IHACRES. Model IHACRES telah membantu menghasilkan anggaran hidrologi yang lebih baik. Model ini digunakan untuk meramalkan aliran sungai ke dalam reservor dan akan digunakan dalam model Vollenweider. Data hujan didapati dari Jabatan Pengairan dan Saliran (JPS) Malaysia bagi stesen 1539001, Loji air Sungai Layang. Sampel air telah diuji dengan menggunakan reagent phos Ver 3 phosphate - DR 4000 (Hach Co. CO 80539-9987, USA) untuk menentukan nilai fosforus terlarut dalam mg/l. Kepekatan fosforus jumlah dari tiga lawatan tapak telah diuji. Nilai purata fosforus jumlah adalah 0.214 mg/l. Kandungan fosforus tertinggi dicerap adalah 0.622 mg/l dan kepekatan terendah adalah 0.053 mg/l. Fungsi keanggotaan fuzzi kemudian digunakan untuk menggambarkan kandungan fosforus, pembebanan hydraulik dan pembebanan fosforus yang mewakili keadaan semasa reservor. Dengan menggunakan fungsi keanggotaan fuzzi, suatu julat anggaran boleh diperolehi. Julat yang paling mungkin berlaku untuk kandungan forfosrus ialah 0.1 mg/l hingga 0.3 mg/l dan untuk pembebanan hydraulik ialah 1350 m/yr hingga 1400 m/yr. Pembebanan fosforus yang dianggarkan ialah 0.26 g/m^2/yr hingga 0.81 g/m^2/yr (7.81 ton/yr hingga 24.28 ton/yr). Purata kandungan fosforus ialah 0.214 mg/l and purata pembebanan hydraulik ialah 1452.25 m/yr. Purata pembebanan fosforus yang dikira ialah 0.6 g/m^2/yr dan berada dalam julat anggaran 0.26 g/m^2/yr hingga 0.81 g/m^2/yr. Nilai bias yang tertinggi untuk simulasi model IHACRES ialah -0.5546 mm/day dan bias yang terkecil ialah -0.0076 mm/day. Nilai R^2 yang tertinggi ialah 0.9925 manakala yang terkecil ialah 0.9208. Kedua-dua statistik ini menunjukkan model ini berfungsi dengan baik. Anggaran bebanan fosforus fuzzi akan dapat membantu penambahbaikan kualilti air tasik dan pengurusan masa hadapan. Untuk mempastikan penurunan tahap fosforus dan keseluruhan kualiti air tasik, pembangunan dan aktiviti kawasan tadahan mestilah diurus dengan betul dam sistematik.

TABLE OF CONTENTS

LIST OF TABLES

LIST OF FIGURES

LIST OF ABBREVIATIONS

Co.	-	Company
Eq.	-	Equation
IHACRES	-	Identification of unit Hydrographs and Component flows from Rainfalls, Evaporation and Streamflow data
Inc.	-	Incorporated
Ltd.	-	Limited
MASMA	-	Manual Mesra Alam
NA	-	Not available
UH	-	Unit hydrograph
Vol.	-	Volume

LIST OF SYMBOLS

A	-	Area
A	-	Event
A_*	-	Crisp set
B	-	Width of each segment
C	-	Mass balance term
CO_2	-	Carbon dioxide
E	-	Evaporation
F	-	Infiltration
f_o	-	Initial infiltration rate
f_c	-	Final infiltration rate
f	-	Temperature dependence of drying rate

	-	Inflow rate
I		
K	-	Coefficient
L	-	Distance of segment from the river side
Lp	-	Annual areal P loading
L_c	-	Critical annual phosphorus loading
NH_3	-	Nitrate
O	-	Outflow rate
O_2	-	Oxygen
	-	Precipitation
P		
P	-	Phosphorus concentration in water
PO_4	-	Phosphate
Q	-	Discharge
Q_o	-	Observed streamflow value
Q_m	-	Modelled streamflow value
q_s	-	Annual hydraulic loading
R	-	Reference temperature
R	-	Runoff
r_k	-	Rainfall
s_k	-	Streamflow
S	-	Condition
S	-	Storage
t	-	Time
t_k	-	Temperature
T	-	Transpiration
T_w	-	Mean residence time of water in lake
u_k	-	Effective rainfall
$U.$	-	Universe
u_o	-	Fixed element
v	-	Velocity
y	-	Depth of river

z	-	Mean depth of lake
τ_w	-	Catchment drying rate at reference temperature
$\mu(x)$	-	Elements x of the universe
Ω	-	Sample space
ω	-	Variable

LIST OF APPENDICES

CHAPTER 1

INTRODUCTION

1.1 Introduction

Water is a basic requirement for life on earth, including human life, crops, livestock and fisheries for our food. Although 70% of the earth surface is covered by water, which seems to be abundance, but not all the resources can be used. Only less than 1% of the total amount is freshwater that is suitable for human use. Water is used in many ways. Often, water is diverted from rivers, lakes, and aquifers to supply domestic, livestock, agricultural irrigation, and various industrial uses (Wurbs and James, 2002).

The management of water resources over a period of time will affect the heath of the people, food security, prosperity of the country and even the future survival. There has been an increase in the awareness related to issues regarding water resources in Malaysia. As the country develops, more water supply is needed for industrial, domestic, agriculture, and energy usages. Economic development is also dependent on the water resources and water supply. Suitable water quality must be reliably supplied for uses in individual homes, farms, and businesses.

Quality and quantity of water is related to each other. Over the years, activities such as excessive development and urbanization, deforestation, and lack of proper management of sewage treatment and discharge has lead to the increase in the

amount of pollution to the rivers. Polluted rivers will reduce the amount of clean water available. If no proper way to overcome the problem, then the country may face water crisis, such as water shortage in the future.

Eutrophication is another aspect regarding the pollution that will affect water quality of the river if it is ignored for sometime. At first, eutrophication is a natural process which will take a long time to happen, but then now the process is accelerated by human activities, which include excessive usage of fertilizer in agriculture, animal feeds, phosphorus components for detergents and other commercial products which contains phosphorus element. Normally after use, most of the phosphorus-contained wastes are just discharged into the environment. This action will enhance the acceleration of the eutrophication rate of a water body such as lake or reservoir (Schnoor, 1996).

Eutrophication is a process leading to over accelerated growth of the algae, causing unpleasant odour, reducing the penetration of sun light, hence reduce the dissolved oxygen inside the water, and this will further lead to the death of the living organism inside the water. The dead organisms will contribute to the increment of the sedimentation process at the waterbed. And finally the water will become unsuitable for usage.

Clean and useable freshwater is a limited source and river is the main source for water supply in Malaysia. The increasing needs of clean water supply plus the shortage of available clean water supply at the same time will post a threat to the community in the country.

1.2 General description of the site

Dams, reservoirs, and relating structures play a key role in water supply and multi-purpose water management. Layang reservoir is selected for this study. This reservoir serves as the water supply for the people around the area, which include Johor Bahru (Sek, 1997).

The Layang reservoir is located near Masai, in Johor Bahru. The reservoir can be divided into 2 parts, which are Hulu Layang reservoir and Hilir Layang reservoir. The activities near the Layang river watershed mostly are villages, plantation and agricultural estates. These areas are most likely to produce wastes and effluents into the Layang river watershed. In other words, these are the sources of potential pollution to the river.

1.3 Objectives of study

The research is done at the Layang catchment area which include the reservoir. The objectives of this study are as follows :

1. To estimate the phosphorus loadings in the Layang reservoir using Vollenweider model.
2. To predict the Layang river inflows into its reservoir using IHACRES model.
3. To incorporate fuzzy membership function in the estimation of phosphorus loadings.

1.4 Scopes of study

1. Selected tools and equipments are used to obtain data for flow rates and water samples at the site. Further testing is done at the laboratory on the water samples with the use of suitable lab equipments to obtain the current phosphorus content of the site area.
2. Simulation of IHACRES model is run to perceive the ability and performance of the model in predicting the streamflow after acquiring all the relevent data.
3. The phosphorus loading of the reservoir can be estimated by using the Vollenweider model after obtaining all the relevant and required data. Fuzzy membership functions are used to describe the range of uncertainty for the estimation of phosphorus loadings.

1.5 Importance of study

Malaysia is one of those fortunate countries in which water resources are abundant. Under normal climatic trends, rain falls almost the entire year in all parts of the country. Although the freshwater resources are renewable, they are also finite and threatened by pollution from industrial, domestic, and agricultural wastes and effluents. One of the consequences of these pollution is the effect on eutrophication. The increase in the phosphorus load to water ecosystems can no longer be compensated by the phosphorus holding capacity of lakes and reservoirs. It is a necessity to manage the hydrological components of water storage, particularly lakes and reservoirs for their optimal use while maintaining an ecological balance. This study is to estimate the phosphorus loadings of the current state of the reservoir and to explore new way of predicting streamflow of the river.

CHAPTER 2

LITERATURE REVIEW

The productivity of a reservoir is always measured by its water quality. The water quality aspects focus on the water pollution problems and determine the ability of a reservoir to perform its function foremost supplying good quality water suitable enough for consumption. Pollutants from human activities have often caused reservoirs to be contaminated. Point and non-point source pollution should be controlled and regulated to improve the quality of the downstream water bodies (Supiah, 2003). The need to understand the quality of reservoirs has long rises attention to scientists and lake managers and to the publics as well. This chapter will focuses on:

i) Water Quality
ii) Nutrient Loadings and Limiting Factor
iii) Nutrient Loading Model – Vollenweider Model

2.1 Water Quality

Originally, the intent of water quality management was to protect the intended uses of a water body while using water as an economic means of waste disposal within the constraints of its assimilative capacity (Davis and Masten, 2004). Humans have depended on water so much that the environmental engineers must

properly design the treatment facilities to remove any pollutants to acceptable levels without effecting the environment. Only by understanding how pollutants from human activities affect water quality, the engineers is able to achieve this purpose and come out with the solution.

2.1.1 Point and Non-Point Sources Pollution

The wide range of pollutants discharge to surface waters can be grouped into two broad classes; point source and non-point source pollution. Point source pollution comes from identified location where waste is discharged to the receiving waters from a pipe or drain such as factories, sewage treatment plants, and oil tankers. Most point source waste discharges are controlled by Department of Environment (DOE) through a works approval and licensing system. The licence for each input specifies the quality and quantity of the waste permitted to be discharged to a river, lake or the sea at a particular location.

Pollution from non-point sources occurs when rainfall moves over and through the ground. As the runoff moves, it picks up and carries away pollutants, such as pesticides and fertilizers, depositing the pollutants into lakes, rivers, wetlands, coastal waters, and even underground sources of drinking water. Pollution arising from non-point sources accounts for a majority of the contaminants in streams and lakes (Zimmerman, 2006). In a surface water body, non-point pollution can contribute significantly to total pollutant loading, particularly with regard to nutrients and pesticides.

Non-point pollution can have significant effects on wildlife and our use of water (Vale, 2006). These effects include:

i) groundwater and surface water contamination
ii) microbiological contamination of water supplies
iii) nutrient enrichment and eutrophication

iv) oxygen depletion

v) toxicity to plant and animal life, including endocrine disruption in fish

2.1.2 Reservoir Eutrophication

Generally, the term "eutrophication" comes from the trophic state of lakes where "eutrophic" means that lakes are high in nutrients supply in relation to volume and dense growths of plankton in the surface waters. Lakes can be divided into three categories based on trophic state; oligotrophic, mesotrophic, eutrophic and hypereutrophic. These trophic descriptions are generally used to indicate the nutrient status of a water body and describe the effects of nutrients on the general water quality and clarity of a water body.

Table 2.1: Lake aging process

Trophic States	
Oligotrophic	• Lakes are generally clear and deep • Low level of productivity due to severely limited supply of nutrients to support algae growth
Mesotrophic	• Waters with more nutrients, and therefore, more biological productivity
Eutrophic	• Waters extremely rich in nutrients, with high biological productivity • They are either weedy or subject to frequent algae blooms
Hypereutrophic	• Extremely eutrophic with high algae productivity and intense algae blooms • Shallow lakes with much accumulated organic sediment

A natural aging process occurs in all lakes, causing them to change from oligotrophic to eutrophic over time. Eutrophication is the response in water due

to over enrichment by nutrients, primarily phosphorus and nitrogen, and can occur under natural or manmade conditions.

In the 1960s, eutrophication was recognized as a major water quality problem affecting many valuable lakes, river, estuaries and coastal areas (Vollenweider, 1987). There was much debate among scientist about the causes of eutrophication. Some considered eutrophication a natural aging process, others thought it involved climatic changes and some believed it was due to increasing pollution. The latter cause was proven to be true and most scientists had agreed that eutrophication was caused from excessive nutrients enrichment of lakes as a result of human activity which has come to be known as “cultural eutrophication”.

Gilliom (1983) defined cultural eutrophication occurred due to the high levels of nutrients that can quickly lead to undesirable growth of algae and other aquatic plants, and to many related water quality problems. Davis and Masten (2004) regarded cultural eutrophication of lakes can occur through the introduction of high levels of nutrients, usually nitrogen and phosphorus, due to poor management of watershed and the input of human and animal wastes. Human settlement in the drainage basin of a lake generally leads to clearing of the natural vegetation, the development of farms and cities. These activities accelerate runoff from the land surface and increase the input of nutrient supply. Also, streams were convenient for disposing of household wastes and sewage, adding to the nutrient load in the receiving water body.

Cultural eutrophication is characterized by an intense proliferation of algae and higher plants and their accumulation in excessive quantities, which can result in detrimental changes in water quality and biological populations and can interfere with human uses of that water body (Fisher et al., 1995). The term eutrophication has been used increasingly to mean the artificial and undesirable addition of plant nutrients, mainly P and N, to water bodies. The perceived negative effects of cultural eutrophication include reduced water transparency and excessive algal and plant growth, which is highly visible and can interfere with uses and

aesthetic quality of water. One consequence of such growths may be taste and odour problems in drinking water. Ecological consequences include hypolimnetic anoxia due to algal decomposition and fish kills and a rapid shift in species composition of the biological community (Cooke et al., 2005). In tropical areas, diseases such as malaria may be enhanced by eutrophication because the insect vector, mosquitoes in the case of malaria, breeds in these waters. Other symptoms of cultural eutrophication are:

i) Early stages symptoms consist of increase in phytoplankton standing crop (biomass) and biomass at other trophic levels
ii) Algal blooms
iii) Complete depletion of oxygen from hypolimnion shortly after stratification occurs: high concentrations of nutrients appear (due to redox reactions)
iv) H_2S, NH_4^+, non-mineralized organic matter, CH_4 found in hypolimnion as a result of anaerobic respiration
v) Invertebrate and fish communities change: species requiring high oxygen levels disappear, species tolerant of low oxygen levels dominate. Species diversity reduced.

2.1.2.1 Eutrophication Process

Traditionally, eutrophication referred only to nutrient loading, its eventual high concentrations in the water column, and the high productivity and biomass of algae that could occur. Organic matter loading may lead to sediment enrichment and loss of volume. Organic matter, whether added to the water column from external or internal sources, also leads to increased nutrient availability via direct mineralization, or through release from sediments when respiration is stimulated by this organic matter and DO is depleted.

Net internal P loading appears to increase exponentially with increasing dissolved organic carbon content of the lake. Allochthonous organic matter contains molecules producing changes in algal and microbial metabolism independently of effects of added nutrients (Cooke et al., 2005). Finally, organic matter added to a lake or reservoir contains energy that is incorporated, in both dissolved and particulate forms, into plant and animal biomass, leading directly to increased living biomass (the microbial loop). Dissolved and particulate organic matter entering the lake or reservoir from streams, wetlands, and from macrophytes, is of great significance to lake metabolism.

Silt may be rich in organic matter and in nutrients sorbed to surfaces of particulate matter. These may become available to algae or macrophytes immediately or at some later time. Silt loading also contributes directly to volume loss and to an increase in shallow sediment area. Whether volume loss is produced by silt deposition or by the build-up of refractory organic matter from terrestrial and aquatic sources, the development of shallow areas fosters further spread of macrophytes and their attendant epiphytic algae. Ultimately these plants promote further losses of DO and release of organic molecules and nutrients as they decay (Figure 2.1).

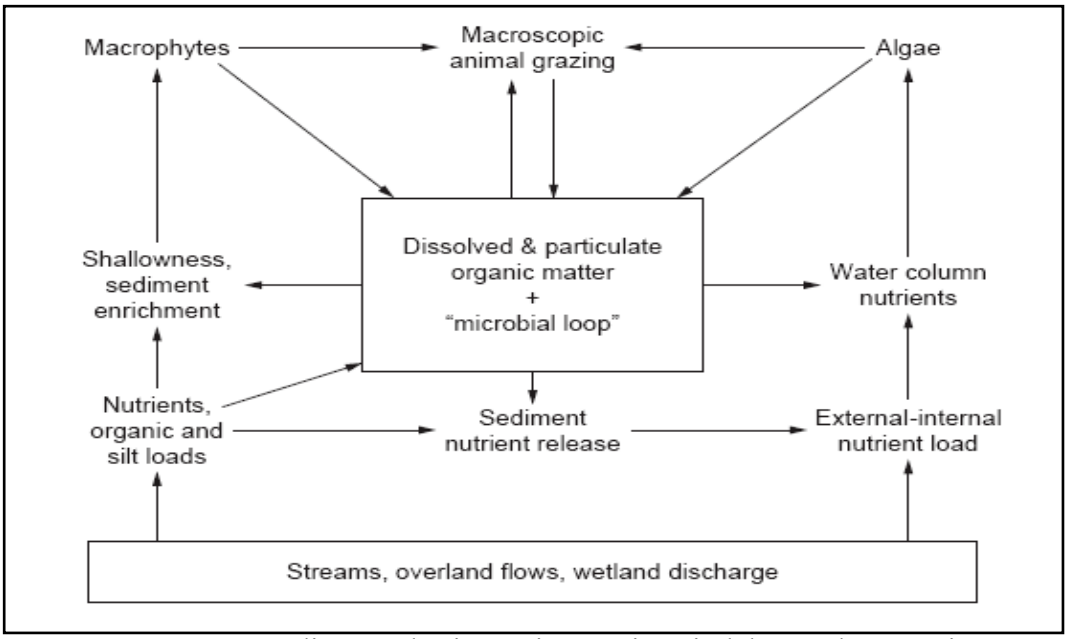

Figure 2.1: Loadings and primary interactions in lakes and reservoirs (Cooke et al., 2005)

Thus, silt and organic loadings have effects on lakes that are additional to their nutrient content, and cannot be excluded when defining the eutrophication process. This view is not meant to downplay or negate the fundamental importance of high nutrient loading in stimulating lake productivity.

Excessive nutrient loading creates potential for eutrophic conditions but does not guarantee increased productivity. Figure 2.1 does not account for the "oligotrophication" effects of high rates of lake flushing and dilution, the effects of organisms in stimulating nutrient release from sediments, or the effects of grazing (or lack of grazing) on algae biomass. Lakes and reservoirs that are naturally eutrophic, or have become so, have characteristics separating them from less enriched and oligotrophic ("poorly nourished") water bodies. Eutrophic lakes have algal "blooms," often of monospecific blue-green (cyanobacteria) populations. Some also have macrophytes, though exotic macrophyte infestations are not a symptom of the eutrophic condition because large populations can develop in oligotrophic waters.

Eutrophic lakes and reservoirs also have colored water (green or brown), and low or zero DO levels in the deepest areas. Warm water fish production is likely to be high. Fish can be limited by low DO and high pH, and lakes may be dominated by less desirable fish species or stunted fish populations.

An oligotrophic lake or reservoir is low in nutrients and productivity because organic matter and nutrient loadings are low or large basin water volumes and short water residence times dilute or pass material through the lake. In addition, high water hardness may foster co-precipitation of calcium carbonate and essential nutrients, rendering them unavailable to algae. Oligotrophic lakes are often deep and steep-sided, with nutrient-poor sediments, few macrophytes, usually no nuisance cyanobacteria, and large amounts of DO in deep water. Water clarity is high, as is phytoplankton diversity, but total algal biomass is low.

2.2 Nutrient Loadings and Limiting Factor

Alteration of the terrestrial landscape by man's activities has usually enhanced the export of materials from the land to rivers and to the atmosphere (Gilliom, 1983). As a result, many lakes, estuaries, and coastal waters experience 'cultural eutrophication' such as increased inflows of particulate and dissolved materials, including N and P which promote the growth of algae if sufficient light is available. Eutrophic aquatic systems often have large accumulations of algae and sometimes macrophyte biomass, although N and P concentrations in the water may be small if algae have assimilated and stored most of the incoming nutrients (Fisher *et al.,* 1995).

2.2.1 Nutrient Loadings

Nutrient loadings concept emerge from total conception that eutrophication happened because of excessive amount of phosphorus (P) and nitrogen (N). The water quality of lake is normally related to total nutrient loading. Eutrophication of aquatic systems results from two sources of nutrient supply; nutrient inputs from outside the aquatic system (external loading), and nutrient recycling within the water column and sediments (internal loading). Natural and anthropogenic processes influence both components of the nutrient supply.

External loading is usually enhanced by man through nutrient inputs to streams and rivers from the fertilization of soils, soil erosion and disposal of municipal or industrial effluents. Atmospheric deposition of both P and N may be enhanced by anthropogenic emissions. The presence of large numbers of animals may also disturb the watershed and increase the nutrient supply to aquatic systems.

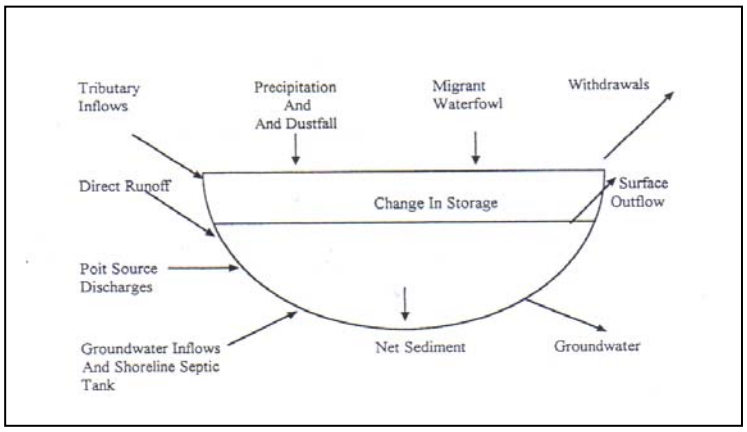

Figure 2.2: Lake Nutrient Budget (Olem and Flock, 1990)

Internal loading results from seasonal or annual return to the water column of nutrients which have sunk and accumulated in sediments, even in undisturbed landscapes with unchanging nutrient inflows. This recycling of nutrients is particularly important in shallow lakes, estuaries and near-shore seas. In deep lakes and ocean basins, nutrient cycling from sediments is less important because of the greater distance between sediments and surface waters (Fisher *et al.,* 1995). The relationship between watersheds, lake processes and water quality responses are described in the lake nutrient budget:

Inflow Loading = Outflow Loading + Net Sedimentation + Change in Storage (2.1)

2.2.2 Limiting Factor

Nutrients are important to plants as it is important to human. Nutrients such as carbon, nitrogen, phosphorus and a variety of trace elements (sufficient quantities) are essential for plants to grow. Alas, too much of these nutrients can

caused uncontrolled growth. By limiting the availability of any one nutrient, further plant growth is prevented (Davis and Masten, 2004).

Macrophyte density, while in part related to sediment type and composition, and to nutrient factors, is often determined by light availability. Long-term control of algal biomass requires significant water column nutrient reduction. Phosphorus (P) is most frequently targeted because it is usually the nutrient in shortest supply relative to demands by algae (the limiting nutrient). Phosphorus does not have a gaseous phase so the atmosphere is not a significant source, unlike nitrogen or carbon. Phosphorus concentration, therefore, can be lowered significantly by reducing loading from land and in-lake sources (Cooke et al., 2005).

There are strong relationships between inputs of P to lakes and the biomass and productivity of phytoplankton (Dillon and Rigler, 1974) which establish the primary importance of phosphorus limitation in freshwater lakes. This conclusion was the basis for the recommendation that reductions in P inputs should be legislated to control eutrophication in Malaysian lakes.

2.2.2.1 Phosphorus

Phosphorus is probably the most studied plant nutrient in freshwater aquatic sciences. It is often found to be (and more often inferred as) the nutrient that limits the growth and biomass of algae in lakes and reservoirs. Phosphorus in natural waters is divided into three component parts: soluble reactive phosphorus (SRP), soluble unreactive or soluble organic phosphorus (SUP) and particulate phosphorus (PP) (Rigler 1973). The sum of SRP and SUP is called soluble phosphorus (SP), and the sum of all phosphorus components is termed total phosphorus (TP). Soluble and particulate phosphorus are differentiated by whether or not they pass through a 0.45 micron membrane filter.

Soluble reactive phosphorus (SRP) dissolves in the water and readily aids plant growth. Its concentration varies widely in most lakes over short periods of time as plants take it up and release it. This phosphorus fraction should consist largely of the inorganic orthophosphate (PO_4) form of phosphorus. Orthophosphate is the phosphorus form that is directly taken up by algae, and the concentration of this fraction constitutes an index of the amount of phosphorus immediately available for algal growth.

Soluble unreactive phosphorus (SUP) contains filterable phosphorus forms that do not react with the phosphorus reagents under the time and conditions of the test. It is measured as the difference between SP and SRP. The compounds in the SUP fraction are organic forms of phosphorus and chains of inorganic phosphorus molecules termed polyphosphates. The size of this fraction relative to the other phosphorus fractions is highly dependent on the type of filter used to separate the soluble from particulate fractions.

Soluble phosphorus (SP) s measured after the digestion of the filtrate and should contain all filterable forms of phosphorus, both organic and inorganic that is converted to orthophosphate by the digestion process. However, the amount of phosphorus in this filterable pool is highly dependent on the filter used. The larger the effective pore size of the filter, the more particulate material that will pass through the filter, be digested, and be considered "soluble."

Total phosphorus (TP) incorporates the total of all filterable and particulate phosphorus forms mentioned above. It is probably the most often analyzed fraction of phosphorus because it is used in a wide variety of empirical models relating phosphorus to a wide variety of limnological variables, and the link between phosphorus loading estimates and phosphorus content in the lake. Total phosphorus is considered a better indicator of a lake's nutrient status because its levels remain more stable than soluble reactive phosphorus. Total phosphorus includes soluble phosphorus and the phosphorus in plant and animal fragments suspended in lake water.

2.2.2.1.1 Phosphorus Cycle

Phosphorus in unpolluted waters is imported through dust in precipitation or via the weathering of rock. Phosphorus is normally present in watersheds in extremely small amounts, usually existing dissolved as inorganic orthophosphate, suspended as organic colloids, adsorbed onto particulate organic and inorganic sediment, or contained in organic water. In polluted waters, the major source of phosphorus is from human activities. The only significant form of phosphorus available to plants and algae is the soluble reactive inorganic orthophosphate species (HPO_4^{2-}, PO_4^{3-}, etc.) that are incorporated into organic compounds.

During algal decomposition, phosphorus is returned to the inorganic form. The release of phosphorus from dead algal cells is so rapid that only a small fraction of it leaves the upper zone of a stratified lake (the epilimnion) with the settling algal cells. However, little by little, phosphorus is transferred to the sediments; some of it in undecomposed organic matter; some of it in precipitates of iron, aluminum, and calcium; and some bound to clay particles. To a large extent, the permanent removal of phosphorus from the overlying waters te the sediments depends on the amount of iron, aluminum, calcium, and clay entering the lake along with phosphorus.

Human activities have led to a release of phosphorus from the disposal of municipal sewage and from concentrated livestock operations. The application of phosphorus fertilizers has also resulted in perturbations in the phosphorus cycle, although these changes are thought to be more localized than the perturbations in the other cycles. Phosphorus releases can have a significant effect on lake and stream ecosystems.

2.2.2.2 Nitrate-Nitrogen

Nitrogen is an element that is found in both the living portion of our planet and the inorganic parts of the Earth system. The nitrogen cycle is one of the biogeochemical cycles and is very important for ecosystems. Nitrogen moves slowly through the cycle and is stored in reservoirs such as the atmosphere, living organisms, soils, and oceans along its way.

Most of the nitrogen on Earth is in the atmosphere. Approximately 80% of the molecules in Earth's atmosphere are made of two nitrogen atoms bonded together (N_2). All plants and animals need nitrogen to make amino acids, proteins and DNA, but the nitrogen in the atmosphere is not in a form that they can use. The molecules of nitrogen in the atmosphere can become usable for living things when they are broken apart during lightning strikes or fires, by certain types of bacteria, or by bacteria associated with legume plants. Other plants get the nitrogen they need from the soils or water in which they live mostly in the form of inorganic nitrate (NO_3^-).

Nitrogen is a limiting factor for plant growth. Animals get the nitrogen they need by consuming plants or other animals that contain organic molecules composed partially of nitrogen. When organisms die, their bodies decompose bringing the nitrogen into soil on land or into the oceans. As dead plants and animals decompose, nitrogen is converted into inorganic forms such as ammonium salts (NH_4^+) by a process called mineralization. The ammonium salts are absorbed onto clay in the soil and then chemically altered by bacteria into nitrite (NO_2^-) and then nitrate (NO_3^-). Nitrate is the form commonly used by plants. It is easily dissolved in water and leached from the soil system. Dissolved nitrate can be returned to the atmosphere by certain bacteria in a process called denitrification.

Certain actions of humans are causing changes to the nitrogen cycle and the amount of nitrogen that is stored in reservoirs. The use of nitrogen-rich fertilizers can cause nutrient loading in nearby waterways as nitrates from the fertilizer wash into streams and ponds. The increased nitrate levels cause plants to grow rapidly until

they use up the nitrate supply and die. The number of herbivores will increase when the plant supply increases and then the herbivores are left without a food source when the plants die. In this way, changes in nutrient supply will affect the entire food chain. Additionally, humans are altering the nitrogen cycle by burning fossil fuels and forests, which releases various solid forms of nitrogen. Farming also affects the nitrogen cycle. The waste associated with livestock farming releases a large amount of nitrogen into soil and water. In the same way, sewage waste adds nitrogen to soils and water.

2.1 Nutrients Loading Models

In view of the complexity of the transport and eutrophication processes, various models have been developed to solve watershed and reservoir problems. Some of them are identified as CREAMS (Chemicals, Runoff and Erosion from Agricultural Management System) developed by Knisel (1980), ANSWERS (Areal Non-point Source Watershed Environment Response Simulation) developed by Beasley et. al. (1980), AGNPS (Agricultural Non-Point Source) developed by Young et al. (1987), QUASAR (Quality Simulation Along Rivers) developed by Whitehead et. al.(1979), VOLLENWEIDER model developed by Vollenweider (1976) and EVENT-BASED STOCHASTIC model developed by Duckstein et. al. (1978). The choice of the models depends on the decision to be made and the problems to be solved (Duckstein et. al. 1978).

The non-point source simulation models vary especially in terms of their temporal and spatial details (Srinivasan, 1992). The model could be used to simulate short term or long term time frame or they could be based on lump or distributed parameter approach. The lump parameter models have a limited spatial details. The lump parameter approach applied block or average watershed physical characteristics for one or more parameters that describe the basin as a whole. The distributed

parameter approach may include spatial variation details in the input parameters and dependent variables. The model which allows for spatial diversity described the watershed behavior comprehensively and is generally more accurate. The major problems in using a distributed parameter approach is to collect all the physically-based data required to drive the model. Besides that they are more computationally intensive and time consuming. For a nutrient relationship study, French (1984) points out that the short term variations are effectively treated by the dynamic distributed models, while the long-term variations in water quality are best addressed by the steady-state empirical lump models. The models that have dominated the non-point modeling arena especially for agricultural areas will be discussed below.

2.3.1 CREAMS

The CREAMS (Chemicals, Runoff and Erosion from Agricultural Management System) model was developed by the United States Department of Agriculture –Agricultural Research Service (USDA-ARS) (Donigian and Wayne, 1991) . This model was developed based on the earlier version initiated by Knisel (1980) for analysis of agricultural best management practices for pollution control. Specifically this physically-based and lumped parameter model was applied for predicting runoff, erosion and chemical transport from field-sized agricultural areas. CREAMS could predict the fate and transport of chemicals in the soil such as total phosphorus and total nitrogen from the agricultural field-sized area. It could also predict erosion, sediment yield, the distribution of the primary sediment particles and sediment-bound nitrogen and phosphorus (Srinivasan, 1992). CREAMS uses a representative slope flow path to describe the field-sized area. The sediment and transport equations will predict the sediment movement for the slope flow path endured. The CREAMS model could determine the storm loads and average concentrations of sediment- associated and dissolved chemicals in runoff (Donigian and Wayne, 1991). The CREAMS model could also simulate the runoff discharges on a daily basis, erosion from field-sized areas and land surface and soil chemical

processes. The CREAMS model could also simulate various management activities which could be defined by the user such as soil incorporation of pesticides, animal waste management, agricultural practices which include minimum tillage and terracing and aerial spraying. CREAMS could be used for long term simulations (usually two to fifty years) and also for simulating single storms.

The CREAMS model consists of three main components; they are hydrologic, erosion or deposition and nutrients movements or chemistry submodels. CREAMS is a product of the agricultural research community with specific emphasis on representing land surface, soil profile and field scale processes (Donigian and Wayne, 1991). CREAMS allows a very detailed representation of the processes involved in estimating nutrient losses in runoff and through leaching. The chemical processes detailed representation include the sorption or desorption, plant uptake, mineralization and nitrification which eventually would control the fate and migration of chemicals in the soil. The land surface detailed representation include the field terraces, drainage systems, field topography and associated sediment erosion processes. Daily erosion and sediment yield, including particle size distribution are estimated at the edge of the field. The detailed hydrologic option is also available which include short term interval rainfall and the popular Soil Conservation Service (SCS) Curve Number procedure. Runoff volume, peak flow, infiltration, evapotranspiration, soil water content and percolation are computed on a daily basis. The structure and the processes involved in the CREAMS model are described in Figure 2.6.

CREAMS advantages and strength are mainly focused on the calibration procedure which are not necessarily required in their modeling effort (Donigian and Wayne, 1991). The model provides an accurate representation of the various soil processes. Most of the CREAMS parameter values are physically measurable. Besides a complex field-sized watershed can be represented with minimum input details when using CREAMS. When the input data needed by the model could not be provided, default values for input variables which are available (except for those describing the slope) can be used for estimating erosion. However, the results

obtained by using the default values will likely be less accurate (Srinivasan, 1992). CREAMS's weaknesses are mainly focused on the variability of the results which could only be represented in the downslope direction and information is not provided during a storm (Srinivasan, 1992). Another weakness of CREAMS is that it is unable to properly simulate areas with a high water tables and a significant interflow component for surface runoff. As CREAMS is a continuous simulation model, the data needed are detail and extensive.

CREAMS has been applied in a wide variety of hydrologic and water quality studies. Sapek and Sapek (1993) studied the application of the CREAMS model to forecast nitrate and chloride leaching from grassland near Warsaw, Poland. Their results ascertained that the CREAMS is a proper tool for forecasting nitrogen balance on permanent grassland, particularly due to nitrate leaching. Gouy and Belamie (1993) applied the CREAMS pesticides transfer submodel at a rainfall simulation scale. The pesticide sub-model of CREAMS was tested to describe the pesticide transfer into runoff generated by a rainfall simulation. Adsorption coefficient, K_d, was found to be a sensitive parameter of the model. Mean K_d measured in the runoff of a rainfall simulation was considerably greater than the reported values (Sapek and Sapek, 1993), especially for the low suspended particle loads. Williams and Nicks (1993) studied the modeling approach to evaluate best management practices for cropland in Durand, USA. The best management practice evaluated was vegetative filter strips, 20m to 30m wide established alongside streams and creeks adjacent to cropland. The studies outcome indicated that filter strips generally reduced sediment and sediment-associated nutrients by 10 to 80% depending on site features and characteristics. Overall filter strips reduced sediment by 56 % and sediment associated nutrients by 50%.

2.3.2 ANSWERS

ANSWERS (Areal Non-point Source Watershed Environment Response Simulation) developed by Beasley et. al. (1980) is primarily a distributed parameter,

event-based-oriented hydrology model as described by Srinivasan (1992). This distributed parameter model is capable of predicting the watershed behavior during and immediately following a rainfall event. ANSWERS is capable of predicting the hydrologic and erosion response of an agricultural watershed limited to a single storm only and not for continuous long term rainfall events. The distributed parameter concept is applied to demonstrate the spatially varying processes of runoff, infiltration, subsurface drainage, and erosion. The distributed parameter approach is applied in the ANSWERS model, where else the lumped parameter approach is used in many other watershed models. ANSWERS is designed to calculate peak flow rates and total surface runoff for single events. It is applied for watershed planning especially for erosion and sediment control on complex and water quality analysis associated with chemicals in sediment. This model was designed for small watershed hydrology with a typical maximum area of 10 square miles. ANSWERS consists of a hydrologic model, a sediment or transport model, and several routing components. The hydrologic model considers infiltration, surface detention, rainfall interception, and surface retention. The erosion component describes the process of soil detachment, transport and deposition (Srinivasan, 1992). Correlation analysis are used for the simulation between the nutrients, sediment yield and runoff volume.

Donigian and Wayne (1991) suggested that the range of element sizes in using ANSWERS are from one to four hectares for a practical application. The model would simulate the hydrological, erosion, transport and deposition processes for each element within the watershed. These processes would include the interception, infiltration, surface storage, surface flow, subsurface drainage, sediment drainage and sediment detachment. The output from previous element then becomes a source of input to the next or adjacent element. Model parameter values are allowed to vary within elements therefore spatial variability within the watershed is easily modified and represented. The runoff and erosion processes are then treated as independent functions of the hydrologic and erosion related parameters (Srivinasan, 1992). One of the major limitations as described earlier on is that the model is only for a single storm event. Besides that, the input data file is quite complex to prepare (Donigian and Wayne, 1991).

Daryoush (1990) applied the ANSWERS model to study the hydrologic responses of an agricultural watershed in southeast Nebraska. The final calibration resulted in a successful representation of the watershed as well as the overall shape of the runoff hydrograph. Results of this study indicated that, generally, nonstructural or agronomic Best Management Practices are effective in controlling erosion and non-point source pollution than structurally-oriented Best Management Practices. The impact of these management strategies on runoff varied considerably. Generally, an intense, short, thunderstorm type of rainfall event had a more relative impact on runoff and sediment yield than a long, gentle, and steady event.

2.3.3 AGNPS

The Agricultural Non-Point Source (AGNPS) model was developed by Young et. al. (1987) of the United States Department of Agriculture - Agriculture Research Service (USDA-ARS) to obtain estimates of runoff quality with primary emphasis on nutrients, pesticides and sediments (Srivinasan, 1992). The AGNPS is a distributed parameter, event-based model that simulates agricultural watersheds by assuming uniform precipitation patterns. The AGNPS model simulates sediments and nutrients from agricultural watershed for a single storm event or for continuous simulation. The basic components of AGNPS are the hydrology, erosion, nutrients and pollutant submodel. The hydrology part applies Soil Conservation Service (SCS) curve number approach and soil erosion part by the Universal Soil Loss Equation (USLE). The pollutant transport portion is subdivided into the soluble pollutants and sediment-based pollutants components. The model is used mainly for comparison purposes, such as comparing the effects of different pollution control practices.

Data needed for the AGNPS model are classified into two categories, watershed and cell data. The watershed data includes information that applies to the entire watershed such as size, number of cells, storm intensity, etc. The cell data will include information on the parameters based on topography, soil type, land use and management practices within the cell. The input data needed are extensive; however,

it could be obtained through visual field observations, topographic and soil maps and from various publications, tables and graphs (Donigian and Wayne, 1991). Meteorologic data consisting of daily rainfall is needed for the hydrologic simulation. The model requires a total of 22 parameters for execution. Output parameters can be examined for a single cell or for the entire watershed. The nutrients, sediment and runoff estimates produced by the AGNPS can be examined for a selected areas within the watershed or for a the whole watershed. In general, AGNPS performed well and provide reasonably satisfactory results.

The equations used to estimate nutrient transport were adapted from the CREAMS model (Frere et al., 1980) and a feedlot evaluation model developed by Young et al. (1982). Nutrients are routed from the watershed either in solution or absorbed into the sediments. The model partitions soluble nitrogen and phosphorus into surface runoff and infiltration pathways. Sediment associated with nutrient yield is estimated using the following equations (Young et.al., 1987):

$$NUTsed = NUT\,st \quad SY \quad ER \tag{2.5}$$

$$ER = 7.4 * Qs^{-0.2\,Tf} \tag{2.6}$$

where,

NUTsed - nutrient either nitrogen or phosphorus transport by the sediment

NUTst - soil nutrient content in the field

SY - sediment yield (kg/ha)

Qs - sediment yield estimated by the sediment routing portion of the model

ER - enrichment ratio

Tf - soil texture correction factor (Young et. al. 1987)

The AGNPS model was further developed by incorporating the Geographic Information System (GIS) - Geographical Resource Analysis Support System (GRASS) interface (Srivinasan, 1992). The AGNPS-GRASS input interface will minimize the user interaction in preparing the input data for the AGNPS model and also minimize the number of user supplied or developed GIS database layers. This

interface will prepare the input data with only 8 basic GIS database layers supplied by the user and with minimal user interaction compared to the 22 different data required by the basic AGNPS model for each cell (Srinivasan, 1992). There are 5 input parameters needed for the whole watershed which will be supplied by the user. The major asset of the GIS approach is that it will automatically extract the required information to calculate the model data. The process of extracting data from the map sources has been divided into two major sections:

i) Topography related data

ii) Soil type and land cover related data.

The topography related variables will include the receiving cell flow direction. The soil type and land cover related data will include the soil erodibility (K) factor, Manning's n and SCS curve number (Srinivasan, 1992).

Table 2.1 : Annual Pollutant Reductions by Different BPMs Scenarios using AGNPS by Mostaghimi et. al. (1997)

Simulation scenarios[a]	Runoff (mm)	Total suspended solids (Mg/ha)	Total N (kg/ha)	Total P (kg/ha)
Pre-BMP conditions	126.9	0.81	20.9	5.08
BMP Scenario 1	115	0.59	14.9	3.44
Percentage reduction[b]	9.4	26.4	31.8	32.1
BMP Scenario 2	123.8	0.68	19.4	4.58
Percentage reduction	2.4	13.5	9.3	9.4
BMP Scenario 3	118.7	0.66	18.1	4.14
Percentage reduction	6.5	17.9	13.3	18.3
BMP Scenario 4	126.9	0.81	14.7	3.72
Percentage reduction	0.0	0.0	29.4	26.6
BMP Scenario 5	123.8	0.68	14.5	3.5
Percentage reduction	2.4	13.5	30.1	30.8
BMP Scenario 6	84.1	0.38	8.37	2.19
Percentage reduction	33.7	52.9	59.8	56.7
BMP Scenario 7	68.3	0.33	7.16	1.66
Percentage reduction	42.6	58.8	65.6	67.2

[a]Scenario 1: combination of BMPs currently installed within the watershed in 1988.
Scenario 2: no-till practice on critical areas (68 ha).
Scenario 3: Conservation Reserve Program (CRP) on critical areas (68 ha).
Scenario 4: animal-waste storage facilities installed.
Scenario 5: no-till on critical areas (68 ha), plus animal-waste facilities.
Scenario 6: no-till cropland (518 ha), plus animal-waste facilities.
Scenario 7: all cropland (530 ha) converted to pasture, plus animal-waste facilities.
[b]Based on the pre-BMP results.

Mostaghimi et. al. (1997) applied the AGNPS model for assessing management alternatives in a small agricultural watershed on the water quality and quantity in the Piedmont Region of Virginia, USA. The runoff, sediment yield and nutrient loadings predicted by the AGNPS model compared favorably with the observed values. A better result was found for runoff but less favorable for peak rates, sediment or nutrient yields. Mostaghimi et. al. (1997) applied the annualization procedure suggested by Koelliker and Humbert (1989) to convert event-based simulation result into a long-term impacts of best management practices (BMPs). The procedure takes into account rainfall amount frequency analysis and the corresponding rainfall erosivity indices. The relative errors of the annualization procedure was 23.5, 14.3 and 8.9 % for sediment yield, nitrate and phosphorus loadings respectively. The model was also used to simulate the effects of seven different BMPs scenarios on the watershed. The reduction rates in simulated pollutant loadings and costs for BMPs implementation were used to identify the appropriate BMPs for the watershed. Their results also indicated that the installation of BMPs on critical areas may be cost effective. The most critical areas could be treated first and then BMPs could be implemented on the less critical areas until the reduction goals are met. The annual pollutant reductions by different BMP scenarios studied by Mostaghimi et. al (1997) are shown in Table 2.1. However, they cautioned that the input data for this model is very time consuming and a lot of difficulties arise in determining the accuracy of the output values.

2.3.4 QUASAR

QUASAR (Quality Simulation Along Rivers) was developed by Whitehead et. al.(1979) to assess the environmental impact of pollutants on river water quality. The model was originally developed with the primary objective of simulating the dynamic behavior of flow and water quality along a river system (Whitehead and Young, 1979). QUASAR performs a mass balance of flow and water quality sequentially down a river system. The model combines inputs from tributaries, groundwater and point and non-point sources to calculate the flow and river water

quality. QUASAR modeled the flow and water quality behavior by dividing the river length into specific reaches. The reach boundaries are determined by points in the river when notable changes in river water quality are observed. The denitrification process within the specific reaches is controlled by a first order temperature dependent rate process. This can be represented mathematically as (Ferrier et. al, 1995):

$$V_r (dN_o/dt) = Q_iN_i - Q_oN_o + Q_rN_r - k_i\, 10^{(0.0293\alpha T)}\, A_r\, N_o \qquad (2.7)$$

where,

N_o - reach output nitrate concentration

N_i - upstream nitrate concentration

N_r - nitrate concentration in rural runoff

Qo - reach output flow

Qi - upstream flow

Qr - rural area flow

k_i - denitrification rate parameter

V_r - reach volume in m^3

A_r - river bed surface area m^2

α - flow rate, $m^3\, s^{-1}$

T - water temperature, ^oC.

QUASAR model could be run in two modes; planning and dynamic modes. In the planning or stochastic mode, cumulative frequency curve and distribution histogram of a water quality parameter are generated by repeatedly running the model using different input data (Ferrier et. al.,1995). In the stochastic or planning mode, the water quality and flow are simulated over a selected period. The water quality and flow data are required in the first reach at the upstream part of the river and tributaries, sewage treatment works discharges, and abstractions at key locations along the river (Whitehead et al., 1984). The simulation procedure run over a selected time period would allow for the possible effects of a pollution event on a river to be investigated. The model is run for every time step, that is the time interval over which the model will dynamically compute river quality and flow. The output

values are used in generating profiles of water quality parameters along the river at a given time or in generating time series data at a specified location. The simulated and observed river flows at the downstream boundary is necessary for the loading estimation. The simulated daily nitrate concentrations and observed monthly are obtained from the study.

Ferrier et. al. (1995) applied the QUASAR model to investigate the impact of land use change and climate change on NO_3-N in the River Don, North East Scotland. They investigated a range of land use scenarios and climate effects to provide a long term view of nitrate nitrogen concentrations in the river in future years. The primary data available for the study were the river reach length and cross section, maximum and minimum temperatures and flow discharges. Flow discharges were monitored continuously at a number of locations on the main river channel by the North East River Purification Board (NERPB), Scotland. Seasonal variations in discharge are apparent, low flows being associated with summer months and high flows as a result of autumn and spring snowmelt. The river water samples were collected approximately monthly over the 11 years period (1980-1990) as part of NERPB's routine water quality control and monitoring duty. Ferrier et. al (1995) identified three reach structure with the non-point inputs along the river system treated as single point input per reach.

2.3.6 Universal Soil Loss Equation (USLE)

The USLE, developed by Wischmeier and Smith (1962) is the most widely used and accepted erosion model (Williams and Hann, 1978). The USLE can be used to predict long-term average annual sediment yields for watersheds by applying a delivery ratio. USLE can also be used for pollution loading estimation by multiplying the sediment yield estimated with the concentration of pollutant in soil. USLE has been used to provide specific and reliable guides for selecting appropriate erosion control practices for farmlands and construction areas (e.g. Morgan, 1986a). This empirically based model, compute soil erosion by assigning values to indices that represent the major factors of climate, soil, topography and land use. Other applications of the equation have been in determining upland erosion for reservoir

sedimentation and stream loading, control of pollution from cropland, and alternative land use and treatment combinations (Morgan, 1986a).

The Universal Soil Loss Equation (Wischmeier and Smith, 1962) expresses the relationship between various factors quantitatively in the following form:

$$A = R.K.L.S.C.P \qquad (2.11)$$

where,

A = mean annual soil erosion loss (tons/ha/year)

R = rainfall erosivity index (tons/ha/ (in/hr))

K = soil erodibility factor (tons/ ha/year per unit R)

L = slope length factor (dimensionless)

S = slope steepness factor (dimensionless)

C = crop management factor (dimensionless)

P = erosion control practice factor (dimensionless)

In metric units,

$$A(\text{tons/ha/year}) = R(\text{J/ha}) \times K(\text{tons/J/year})\ LSCP \qquad (2.12)$$

Note: ha - hectar

J - Joule (Nm or kg m^2/s^2)

The soil erodibility factor, K is a measure of the susceptibility of soil particles to the detachment and transport process by rainfall and runoff. K is a quantitative description of the inherent erodibility of a particular soil. The principle factor affecting K is the soil properties, structure, organic matter and permeability. Representative values of K for most of the soil types and texture classes have been compiled by the Soil Conservation Service, USA (Morgan, 1986a).

Slope length or topographic factor, LS is defined as the distance from the point of origin of overland flow to the point where the slope decreases sufficiently for deposition to occur or to the point where runoff enters a defined channel (Singh, 1992). The LS factor describes the combined effect of slope length and slope gradient. The LS factor is also defined as the ratio of soil loss per unit area on a site to the corresponding loss from a 22.13m long experimental plot with a 9% slope.

Slope gradient in the field or segment slope is usually expressed as a percentage. The development of segment slope was based on a standard plot length of 22.13 m (Wischmeier and Smith, 1962).

The cover and management factor, C is defined as the ratio of soil loss from land under specified crop or mulch conditions to the corresponding loss from tilled and bare soil. This cropping management factor represents the ratio of soil loss from a specific cropping or cover condition to the soil loss from a tilled, continuous fallow condition for the same soil, slope and same rainfall (Wischmeier and Smith, 1978). This factor measures the combined effect of all the interrelated cover and management variables including the type of vegetation, plant spacing, the stand, the quality of growth, crop sequence, tillage practices, crop residues, incorporated residues, land use residue and fertility treatments (Singh, 1992). Crops can be grown continuously or rotated with other crops. Soil loss and sediment yield can be reduced if the particular site is covered with vegetation. The greatly expanded tables of C factor values were presented by Wischmeier (1960), Wischmeier and Smith (1962), Roose (1977) and Morgan (1986a).

Support practice factor, P is defined as the ratio of soil loss with a given surface condition to soil loss with up and down hill culture (Wischmeier and Smith, 1978). Important cropland practices are contour tillage, strip cropping on the contour and terrace systems. Practices that reduce the velocity of runoff and the tendency of runoff to flow directly down slope reduce the P factor. Since slope length influences the effectiveness of contouring, the P values are based on maximum slope lengths. Mitchell and Bubenzer (1980) indicated conservation tillage, crop rotations, fertility treatments and the retention of residues are important erosion control practices. They also indicated that the P factor is most effective for the 3-8% slope range and values increase as the slope increases.

USLE had been modified and renamed in several versions such as MUSLE (Modified Universal Soil Loss Equation) and RUSLE (Revised Universal Soil Loss Equation). The USLE was not designed for application to individual storms and is

therefore, not appropriate for individual storm water quality modeling. The USLE was modified by Williams (1975a) for watershed application by replacing the rainfall energy factor with a runoff factor. This modified version called MUSLE increased sediment-yield-prediction accuracy, eliminated the need for delivery ratios, and is applicable to individual storms. The MUSLE was combined with the modified SCS water-yield model to form a daily runoff-sediment prediction model (Williams and Berndt, 1976). The MUSLE is useful in predicting sediment yield from small watersheds (< 40 km^2) however sediment routing is needed to maintain prediction accuracy on large watersheds with non-uniformly distributed sediment sources (Williams and Hann,1978). A sediment routing model was developed for large agricultural watersheds (Williams, 1975b) and has had limited testing.

Although USLE was widely used, it has some important limitations. The data base used in developing the USLE was collected on the east of the Rocky Mountains, therefore its limitation when applying in the other parts of the world especially in the arid and tropical region must be recognized (Simons et. al.,1982). Many arid regions in the western United States gets a large percentage of rainfall in the form of high intensity, short-duration thunderstorms. As this in not the case in the eastern United States, the effect of this type of rainfall cannot be totally incorporated. The USLE can be helpful for prediction of sediment contributions from these sources to downstream water bodies, but the limitations in terms of the type of erosion applicable must be recognized. The USLE is designed to predict average annual soil loss by sheet and rill erosion on unsloped areas such as farmland and agricultural areas. Its predictions do not include sediment contributions from gully erosion or landslides. Since it was designed for sheet and rill erosion, it should not be used to estimate sediment yield from drainage basins. The soil loss estimated using USLE does not include factors to account for sediment losses or gains between the field and stream or reservoir. These items must be evaluated separately. The USLE was developed from data taken from small plots. Because of its regression nature, results become suspicious when applied to much larger areas. It has been developed for materials in the range of 1mm or finer, and does not predict the yield of larger sediment sizes (Simons et. al, 1982).

2.3.7 Event-Based Stochastic Model

The Event-Based Stochastic Model was developed by Duckstein et. al. (1978) for phosphorus loadings estimation. This Event-Based Stochastic Model recognized the stochastic nature of nutrient input and the probabilistic description of phosphorus loadings in terms of their frequency and the uncertainty (Duckstein et. al. 1978). The model encoded the uncertainty of phosphorus loadings in terms of mean, variance and probability density function. The model accounts separately the two different forms of phosphorus; dissolved phosphorus and sorbed phosphorus. Phosphorus input is separated into the two components to account for the two different forms of transport of phosphorus from the watershed into the lake.

The elements of the Event-Based Stochastic Model are summarized as follows:

i) Random precipitation events which lead to transport of phosphorus by the two associated mechanisms (runoff volume and sediment yield)

ii) Source of phosphorus, dissolved and sediment phosphorus for a given watershed

iii) Dissolved phosphorus loadings, a function of runoff volume

iv) Sediment or particulate phosphorus loadings, a function of sediment yield

v) Total seasonal loadings of dissolved phosphorus and sediment phosphorus.

This Event-Based Stochastic Model is further elaborated in Chapter 4.

2.3 Nutrient Loading Model

There are several research and method that contributes to the development of nutrient loading evaluation. The most useful and extensively being used is the model introduced by Richard A. Vollenweider. The model has been widely applied in many studies because of its proper definition of lake eutrophication process.

2.3.1 Vollenweider Model

The Vollenweider Model is a useful tool in determining the trophic state of water body based on phosphorus loading (P-loading) and the water depth. The model was originally developed for application to deep, glacial lakes located in the northern hemisphere (Vollenweider, 1968). Vollenweider radically changed our view of lakes when he emphasized the importance of nutrient inputs from the watershed in the determination of the concentration of nutrients and, ultimately, the density of algae in the lake. He was able to convince a new generation of limnologists to look to the watershed to understand the lake only after 50 years later.

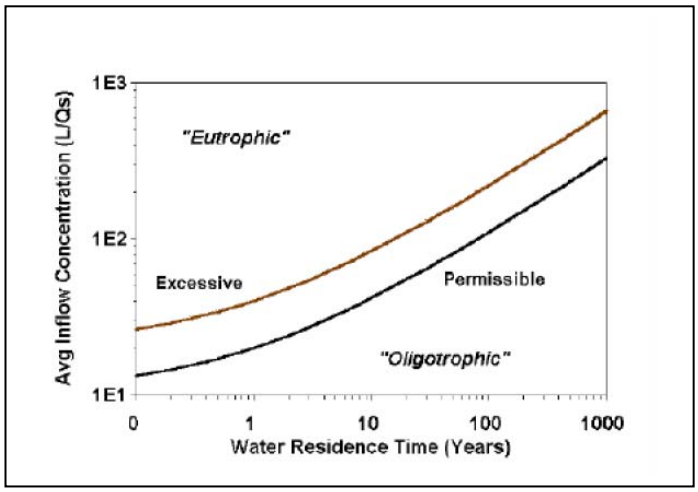

Figure 2.5: Vollenweider loading graphs

A series of loading graphs of Vollenweider appeared to support the idea that trophic state should be directly related to loading. Figure 2.5 illustrates how

investigators with loading data are tempted to simply classify the trophic state of a lake. In this case, trophic state is determined by plotting "Average inflow concentration," which is calculated by dividing loading (L) by water loading (q_s), against hydrologic constraints (water residence time). The “Permissible” line is the boundary between oligotrophy and mesotrophy, and “Excessive” line, the boundary between mesotrophy and eutrophy (Vollenweider 1976).

The Vollenweider model is based on a five year study involving the examination of phosphorus load and response characteristics for about 200 water bodies in 22 countries in Western Europe, North America, Japan and Australia. Vollenweider, working on the Organization for Economic Cooperation and Development (OECD) Eutrophication Study, developed a model describing the relationship of phosphorus load and the relative general acceptability of the water for recreational use. He found that when the annual phosphorus load to a lake is plotted as a function of the quotient of the mean depth and hydraulic residence time, lakes which were eutrophic tended to cluster in one area and oligotrophic lakes in another (Vollenweider, 1975).

Vollenweider developed a statistical relationship between areal annual phosphorus loading (Lp) to a lake normalized by mean depth (Z) and hydraulic residence time (T), to predict lake phosphorus concentration (P). The general steady-state equation for phosphorus loading by Vollenweider (1976) can be written as:

$$L_p = \sum_{i=1}^{n} Q_i [P]_i + L_{INT} \qquad (2.1)$$

where

L_p is the loading of phosphorus per unit area per year ($mgm^{-2}yr^{-1}$)

Q_i represents the amount of water supplied by each input

P_i is the mean P concentration of dissolved and sediment-bound phosphorus (external loading)

L_{INT} is the loading from the lake sediments to the water column (internal loading)

Internal loadings of P from lake sediments to the water column are difficult to measure. Assuming negligible L_{INT}, the equation becomes:

$$L_p = P_{tot} \cdot q_h \cdot \left(1 + \sqrt{T_w}\right) \tag{2.2}$$

where

L_p is the loading of phosphorus per unit area per year ($mgm^{-2}\ yr^{-1}$)

P_{tot} is the mean P concentration of dissolved and sediment phosphorus in the water body

q_h is the hydraulic loading (myr^{-1})

T_w is the mean residence time of water in the lake (yr)

As a general rule, the critical P values that will convert the oligotrophic state to the mesotrophic state is $10 \mu g / L$. Thus the equation (2.2) can be transformed into:

$$L_c = 10 \cdot q_h \left(1 + \sqrt{z / q_h}\right) \tag{2.3}$$

where

z is the lake mean depth (m)

The phosphorus loading Y tons $year^{-1}$ is obtained by multiplying the loading L tons $m^{-2}\ yr^{-2}$ with the surface area of the reservoir.

CHAPTER 3

METHODOLOGY

3.1 Site description

The Layang reservoir in Layang catchment area can be divided into two reservoirs, which are Hulu Layang reservoir and Hilir Layang reservoir. The reservoir is located in Masai, around 40 km travel distance from Johor Bahru city. The maximum altitude is 160 m while minimum altitude is 30 m above the mean sea level. The areal coverage for the catchment area approximately yields within coordinates of latitudes 1^{o} 30' N until 1^{o} 36' N and longitudes 103^{o} 50' E until 104^{o} 00' E.

Hilir Layang reservoir is situated on the east side of Hulu Layang reservoir. The drainage basin for Hilir Layang reservoir is 20.5 km^2. The total drainage basin for both Hulu and Hilir reservoir is 50.5 km^2. The water outflow from both catchments is approximately 40 mega gallons per day. The outflow rate of water from the intake tower to the water treatment plant is 28.5 mega gallon per day (Sek, 1997).

The activities near the Layang river watershed mostly are villages, plantation and agricultural estates. These areas are most likely to produce wastes that will contribute to the discharge into the Layang river watershed when large amounts of fertilizers and pesticides were used in these areas. In other words, these are the

sources of potential pollution to the river that contains high phosphorus concentration. The agricultural activities and palm oil plantations cover most of the watershed area, while the primary forest only occupy a small part of the area.

Table 3.1 : The settlements within Layang river watershed
(Health Department, 1996)

Hulu Layang reservoir	Kampung Penorogo Felcra Ban Foo Ladang Plentong
Hilir Layang reservoir	Ladang Keck Seng Ladang Bulkit Layang Ladang Sungai Tiram

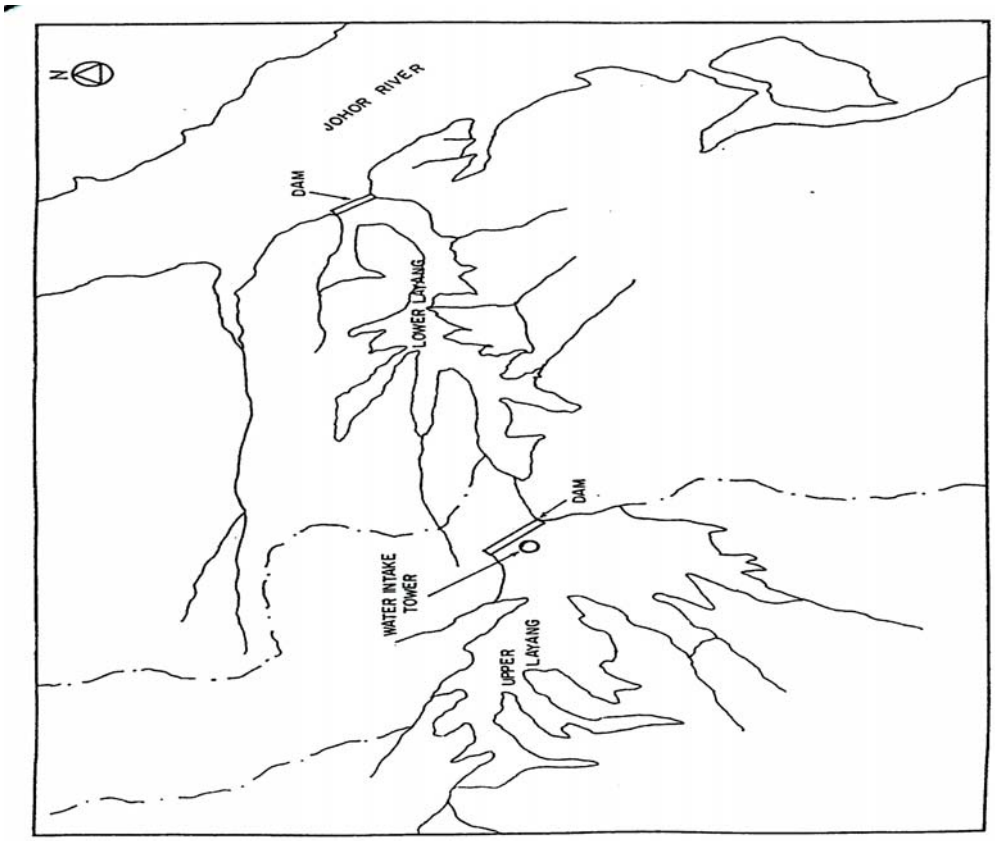

Figure 3.1 : Location of Layang reservoir

3.2 Research design

For the preliminary research, the selected models were studied and understood of its functions. After gaining understandings of its parameters, then the data collection process can began. The data that need to be obtained are precipitation, temperature, streamflow, and phosphorus content. Then, the data is analysed to ensure its continuity and refill the missing data. The precipitation, temperature, and streamflow serve as basic requirement for the IHACRES model. After the streamflow is computed by IHACRES, then it is used together with the phosphorus content data in the Vollenweider model. The phosphorus loadings are computed using fuzzy membership function to obtain a range of the estimated values.

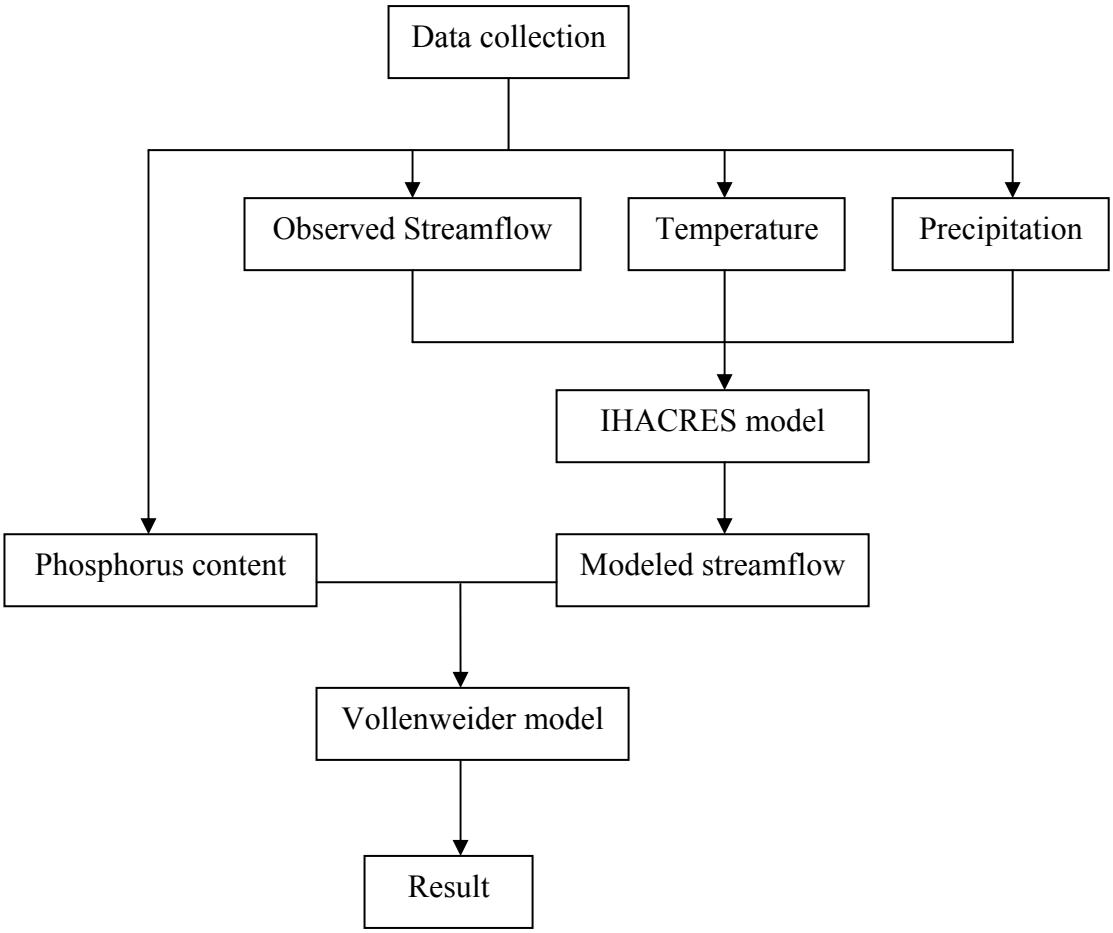

Figure 3.2 : Flow chart of methodology

3.3 Data collection

For the purpose of this study, visitations will be made to the site to take measurements and to obtain the water samples for testing. Three visits were launched to the site with the help from technical assistants of hydraulic and hydrology department. The visits were conducted on 21/12/2006, 10/01/2007 and 21/02/2007.

3.3.1 Water sampling

Water samples can be taken with the help of a tool called water sampler. The commonly used water sampler consists of a cylindrical tube with a stopper on each end that is controlled by a closing device. Water sampler can be used to take water samples at any desired depths, which make it handy when the stream or river only can be reached from higher grounds for example bridges. In order to use it, the tube is lowered into the water at the desired depth with the rubber plugs open. A weight is then dropped down the supporting cord to trip the closing mechanism, which will close the stoppers and trap water inside the tube.

3.3.2 Streamflow measurement

The velocity-area method is used in this study to determine the streamflow of the river. In order to use this method for the determination of discharge, measurements of stream velocity, depth of flow and the distance across the

channel between observation verticals are needed. The velocity is measured at one or more points on each vertical in each segment by using a current meter and an average velocity is determined in each vertical. The discharge is derived from the sum of the product of mean velocity, depth and width of the segments.

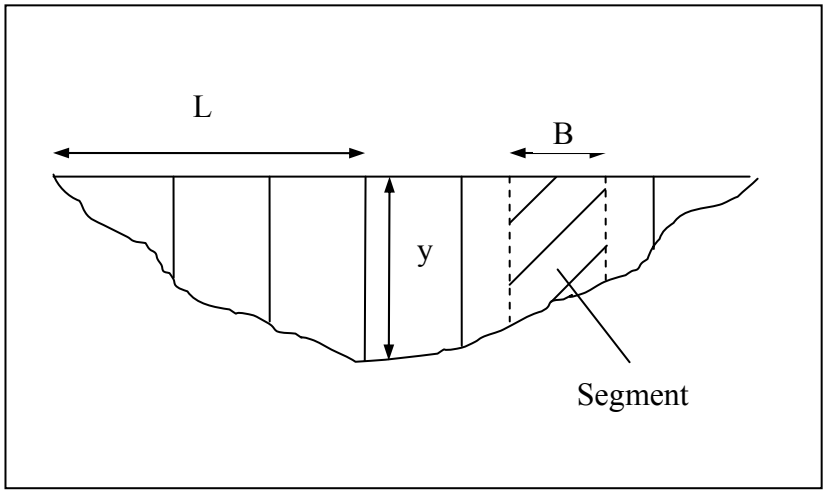

$$Q = \sum v \,.\, A$$
$$= \sum v \,.\, B \,.\, y$$
$$= \sum v \,.\, (L_n - L_{n-1}) \,.\, y \qquad \text{[Eq. 3.1]}$$

where Q is the discharge (m^3/s)

v is the velocity (m^2/s)

A is the area of the segment (m^2)

B is the width of each segment (m)

y is the depth of river (m)

L is the distance of segment from the river side (m)

In the mid section method of computation it is assumed that the velocity sampled at each vertical represents the mean velocity in a segment. The segment area extends laterally from half the distance from the preceding vertical to half the distance to the next, and from the water surface to the sounded depth as shown by

the hatched area in figure. The segment discharge is then computed for each segment and these are summed to obtain the total discharge (Herschy, 1995).

3.3.3 Phosphorus testing

The water samples taken from site were brought back to the lab for testing of the phosphorus concentration in the water samples. The samples were tested using reagent phosVer 3 phosphates and DR4000 spectrophotometer (Hach Co. CO80539-9987, USA). The phosphorus content is indicated in mg/l.

3.4 Vollenweider model

From studies and research by many researchers in the past, they discovered that the phosphorus is the limiting nutrient in a lake. Therefore, a mass balance for this limiting nutrient can be developed. The total phosphorus takes into account of the entire phosphorus element that exist in the lake, including organic, inorganic, dissolved, and even particulate forms of phosphorus in the water. The lake can be assumed to be a completely mixed system by the condition of steady flow and its constant volume. The average concentration of total phosphorus in the lake is equal to the concentration in the outflow (Schnoor, 1996).

$$\text{Accumulation} = \text{Inputs} - \text{Outputs} - \text{Sedimentation}$$

This simple mass balance has become a basis for many researches regarding eutrophication dating back to the work of Vollenweider in 1969.

Vollenweider developed one of the most practical models in 1968 based on comparative studies of European and North American lakes. In this model, the trophic status of a lake is a function of the rate of areal nutrient supply, basin form and flushing rate in the form of mean depth / hydraulic residence time. Hydraulic residence time is the time required to fill a lake at present rates of inflow. Since it is impossible in any practical sense to manipulate mean depth or hydraulic residence time, this model was used to predict the likely effects of altering the rate of nutrient supply on lake trophic status.

$$Lp = P \,.\, qs \,.\, (1 + \sqrt{T_w}) \qquad \text{[Eq. 3.1]}$$

where Lp is the annual areal P loading ($mg/m^2/yr$)

P is the phosphorus concentration in water (mg/l)

q_s is the annual hydraulic loading (m/yr)

T_w is the mean residence time of water in lake (yr)

The commonly accepted, critical phosphorus concentration that will convert the lake from oligotrophic to mesotrophic is 10 mg/m^3. Therefore, Equation 3.1 can be written as:

$$L_c = 10 \,.\, q_s \,.\, (1 + \sqrt{z/q_s}) \qquad \text{[Eq. 3.2]}$$

where Lc is the critical annual phosphorus loading ($mg/m^2/yr$)

z is the mean depth of lake (m)

3.5 IHACRES

3.5.1 Overview

The rainfall runoff model used in this study is the IHACRES model that was developed collaboratively by Institute of Hydrology in United Kingdom and the Centre for Resource and Environmental Studies of Australian National University in Canberra. The IHACRES model software can be downloaded at www.toolkit.net.au/ihacres. The program operates on Java platform and therefore must have Java Runtime Environment installed first.

IHACRES stands for Identification of unit Hydrographs and Component flows from Rainfalls, Evaporation and Streamflow data. IHACRES is a catchment-scale rainfall-streamflow modeling methodology. Its purpose is to assist the hydrologist or water resources engineer to characterise the dynamic relationship between basin rainfall and streamflow.

In order to run the simulation with IHACRES, the model must be calibrated first to obtain a small set of parameters as characteristics to represent the catchment area. This is done to optimise the performance of the model over a known period of time. The inputs of the model will be a time series of rainfall, either temperature or potential evapotranspiration. The output of the model will be a time series of modelled streamflow. The observed streamflow will also serve as a input. This particular data will be used for the calibration period and validation period. Hence, the performance of the model can be computed.

The calibration function of the model has two modules in series, which are a non-linear loss module and a linear unit hydrograph module. The linear relationship between effective rainfall and streamflow enable the unit hydrograph (UH) theory to be applied. The catchment is conceptualised as a configuration of linear storages acting in series and or in parallel. All of the non-linearity which normally observed

between rainfall and streamflow is accommodated in the non-linear loss module that converts rainfall to effective rainfall.

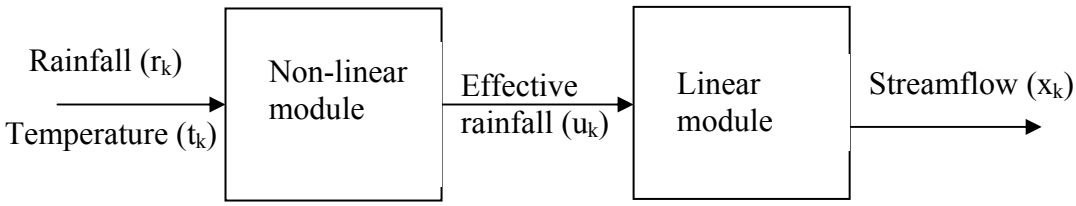

Figure 3.4 : The system structure of the rainfall – runoff model

Conceptualising the spatially distributed processes in both the non-linear and linear modules is restricted. An advantage of this spatially "lumped" approach is that the model requires only a few parameters, where three for the non-linear module and three for the linear module. Although it convey some extent of simplicity, the IHACRES methodology performs well for many types of catchments (Evans and Jakeman, 1998).

3.5.2 The non-linear module

The part of model where all the non-linearity in the catchment scale rainfall-runoff process is accounted for is the effective rainfall component. Effective rainfall is the part of rainfall that leave the catchment area as streamflow. A catchment that contains more moisture will generate more streamflow from a rainfall compared to the time when the catchment is dry. This observation in employed in the form of catchment wetness index, s_k and effective rainfall, u_k. The effective rainfall is a product of rainfall, r_k and the catchment wetness index, s_k (Jakeman and Hornberger, 1993).

$$u_k = r_k s_k \quad \text{[Eq. 3.3]}$$

$$s_k = Cr_k + \left(1 - \frac{1}{\tau_w(t_k)}\right) s_{k-1}, \quad s_0 = 0 \quad \text{[Eq. 3.4]}$$

$$\tau_w(t_k) = \tau_w e^{0.062f(R-tk)}, \qquad \tau_w(t_k) > 1 \quad \text{[Eq. 3.5]}$$

where u_k is the effective rainfall

r_k is the rainfall

s_k is the catchment wetness index

C is the mass balance term

τ_w is the catchment drying rate at reference temperature

t_k is the temperature

R is the reference temperature

f is the temperature dependence of drying rate

Parameter τ_w is the value of $\tau_w(t_k)$ at a reference temperature chosen by the user. In equation 3.4, $\tau_w(t_k)$ controls the rate at which the catchment wetness index decays in when there is no rainfall events. Parameter f controls the sensitivity of $\tau_w(t_k)$ to changes in temperature. For time intervals with rain, decay of catchment wetness index still occurs but it is also incremented by a proportion mass balance term of the rainfall. Value for parameter C is selected so that the volumes of effective rainfall and observed streamflow over the model calibration period are equal. This value is calculated automatically during the model calibration.

3.5.3 The linear module

In a simple discrete-time hydrograph, a unit of effective rainfall over one data time step is considered to produce streamflow ($b < 1$) over the same time step. The effective rainfall and flow is zero in the previous time step and effective rainfall is zero in all following time steps. In each following time step, streamflow is a fixed

proportion (a < 1) of what it was in the previous time step and the flow will reduce exponentially.

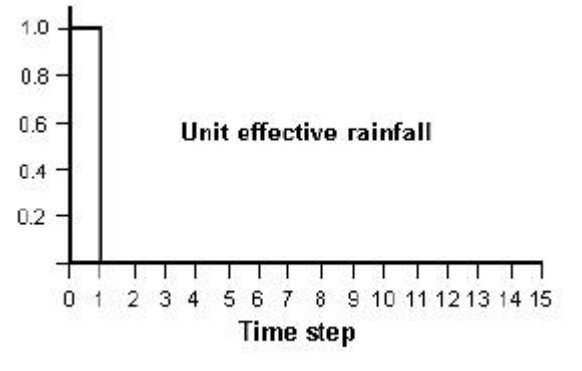

Figure 3.5 : Unit effective rainfall

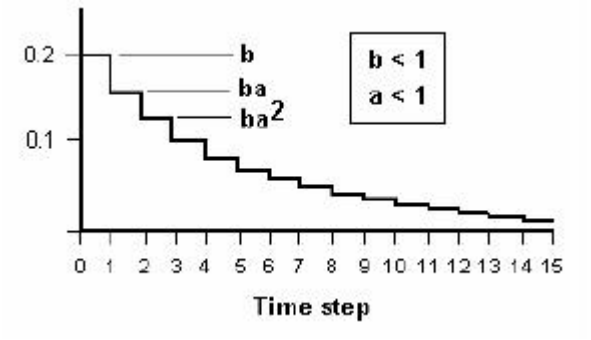

Figure 3.6 : Resultant unit hydrograph

The area under the resultant UH is the sum of the infinite geometric series ($b + ba + ba^2 + ba^3 + ...$). With $0 < a < 1$, this infinite geometirc series sums to $b / (1 - a)$. The shape of this simple UH is completely defined by 1 parameter, either a or b.

$$b (1 + a + a^2 + a^3 + ...) = b / (1 - a) \qquad \text{[Eq. 3.6]}$$

$$b = 1 - a \qquad \text{[Eq. 3.7]}$$

Convolution of the UH with effective rainfall excess (..., u_{k-2}, u_{k-1}, u_k, u_{k+1}, u_{k+2},...) to estimate streamflow (..., x_{k-2}, x_{k-1}, x_k, x_{k+1}, x_{k+2}, ...), can be executed by recursive application of Equation 3.8.

$$x_k = ax_{k-1} + bu_k \quad \text{[Eq. 3.8]}$$

Theoretically, the catchment-scale rainfall-runoff process can be represented by any number of these simple UHs in series and/or parallel. In practice, the IHACRES methodology shows that usually two UHs in parallel is the optimal configuration identifiable from the rainfall, streamflow and temperature data (Evans and Jakeman, 1998). So in this case, the exponential reduction rates for the two simple UHs are describe as quick(q) and slow(s). Total streamflow is the sum of the two separate UHs. In this case, Equation 3.9 applies and the linear module has three parameters, which come from any three of $a^{(q)}$, $b^{(q)}$, $a^{(s)}$ and $b^{(s)}$.

$$[b^{(q)} / (1-a^{(q)})] + [b^{(s)} / (1 - a^{(s)})] = 1 \quad \text{[Eq. 3.9]}$$

The quick and slow components of streamflow are estimated using Equations 3.10 and 3.11 respectively. The total streamflow, x_k is calculated by Equation 3.12.

$$x_k^{(q)} = a^{(q)} x_{k-1}^{(q)} + b^{(q)} u_k \quad \text{[Eq. 3.10]}$$

$$x_k^{(s)} = a^{(s)} x_{k-1}^{(s)} + b^{(s)} u_k \quad \text{[Eq. 3.11]}$$

$$x_k = x_k^{(q)} + x_k^{(s)} \quad \text{[Eq. 3.12]}$$

The two UHs in parallel structure describe that the streamflow hydrographs for natural flow regime are basically the combination of baseflow, which can be noticed during periods of no effective rainfall and runoff responses, which caused by the effective rainfall events.

3.5.4 Data requirement

3.5.4.1 Input data

IHACRES requires three sets of time series data as the input, which are:

- Observed rainfall (in mm or inches)
- Temperature (in degree Celsius, Fahrenheit, or Kelvin) or evapotranspiration (in mm or inches)
- Observed streamflow (in m^3/s, megalitres per time step, millimetres per time step, l/s, or cubic feet per second).

The source of data must be in delimited ASCII text format. Each time series of the required data can be stored in one file with three separate columns for each type of data or in three different files for each data.

The timesteps of the time series supported are in minutes, hours and days. Catchment area in km^2 may be required depend on the measurements units used for the observed streamflow data.

3.5.4.2 Calculated data

After the simulation, a time series of modelled streamflow will be produced, along with multiple statistics which describe the characteristics of each series. Almost all of the data and tables can be exported as comma delimited ASCII text files. Graphs are also viewable in the program.

The results of the grid searches done during calibration can be saved as .igs files which can later be reopen for reuse. After the data has been loaded and a project is created, the project file can be saved as a project (.ipr) file.

3.5.5 The three modes of operation

3.5.5.1 Data

Each component has its own sets of tabs to serve as its own function. The data component has three tabs which are:

- Summary - a summary of that data that is loaded
- Import - a tool to load the time series data as input
- View - a tool to review the loaded data in graph form

3.5.5.2 Calibration of a model

The calibration mode has two tabs which are:

- Model - to build the model by both linear and non-linear modules
- Periods - to define the calibration periods

The calibration period will have to be set first before the calibration of the model can be executed to obtain the parameter sets.

3.5.5.3 Simulation

Simulation cannot be run before the calibration process is completed. After the calibration process, simulation is run to obtain the modelled streamflow time

series. The modelled streamflow time series results can be explored through the tabs available which are the calibration, simulation summary, statistics summary, charts and hydrograph.

3.6 Fuzzy Logic

Fuzzy logic is a method to deal with imprecision or approximation in reasoning. All truths in fuzzy logic are either partial or approximate, unlike in classical logic where the truth is either completely true or completely false. Interpolative reasoning is the terms used to represent the process of interpolatting between the binary extremes of true or false to determine the partial truth in fuzzy logic. (Ross, 2004)

> Fuzzy logic allows for set membership values to range between 0 and 1. Implementation of imprecise concepts such as "slightly" and "very" in the data set can be made, which eventually related to fuzzy sets and possibility theory. It was introduced by Lotfi Zadeh at the University of California, Berkeley in 1965 (http://en.wikipedia.org/wiki/Fuzzy_logic, 05/03/2007).

Application of fuzzy logic has increased after it was applied commercially in 1987 by Matshushita Industrial Electric Co., a company that used the logic in a shower head that controlled the water temperature. Most of the application of fuzzy logic can be seen in the control system of electronic appliances or products, such as washing machines, refrigerators, air conditioners, cameras, and automobile subsystems (http://www.bartleby.com/65/fu/fuzzylogi.html, 05/03/2007).

3.6.1 Fuzzy membership function

Decisions making in processes that contain certain degree of uncertainty has been shown to be less than perfect. Set membership is the key to decision making when faced with uncertainty (Ross, 2004). All information contained in a fuzzy set can be described by its membership function. The membership of an element may be measured by a degree, which also known as the membership degree of that element to the set. The value will range within the interval of [0,1] by agreement (Galindo et al., 2006).

The region in the universe of a typical fuzzy set consists of the core, support and boudaries. The core of a membership function is the region of the universe that is characterized by complete and full membership in the set. The core is made out of the element x of the universe, μ so that $\mu(x) = 1$. The support of a membership function is the region of the universe that is characterised by nonzero membership in the set. The support made of other elements x of the universe so that $\mu(x) > 0$.

The boundaries of a membership function is the region of the universe which contain elements that have a nonzero membership but not complete membership. The boundaries comprise those elements x of the universe such that $0 < \mu(x) < 1$. These elements of the universe are those with some degree of fuzziness, or only partial membership in the fuzzy set.

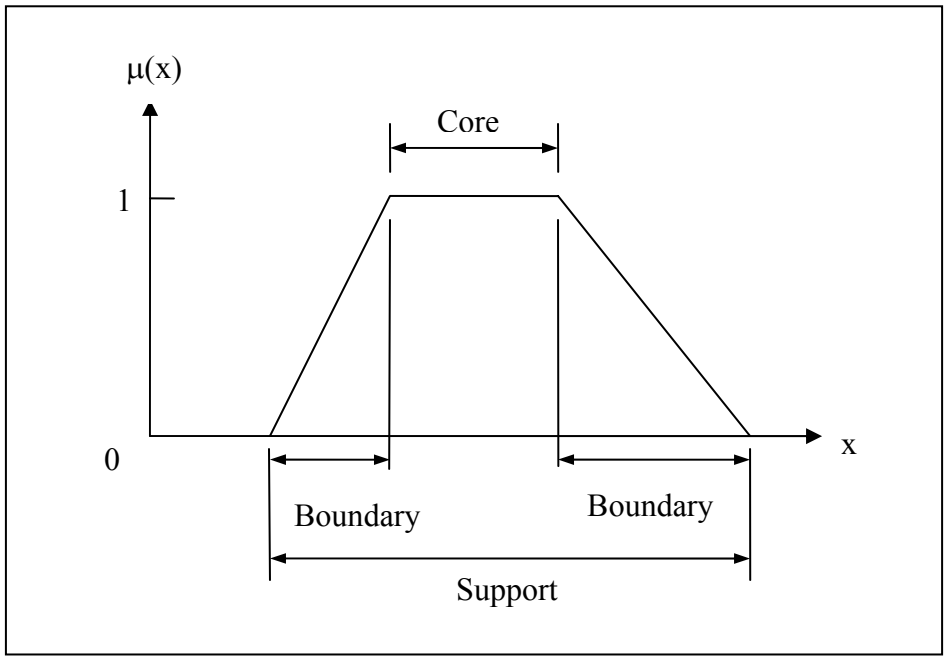

Figure 3.22 : The features in a fuzzy membership function

3.6.2 General method to determine membership functions

There are different kinds of phenomenas that would happen around us. These phenomenas can be divided into two types, which are phenomena of certainty and phenomena of uncertainty. The uncertain phenomena can then be further subdivided into random or stochastic phenomena and fuzzy phenomena (Hong and Vincent, 1995).

Therefore, three categories of phenomena can be identified, together with their related mathematical models:

1. Deterministic mathematical models - where the relationships between objects are known with certainty.

2. Random (stochastic) mathematical models - where the relationships between objects are uncertain or random in nature.
3. Fuzzy mathematical models - where objects and relationships between objects are fuzzy.

The main difference between random phenomena and fuzzy phenomena is that the random events have well-defined meaning, while fuzzy concept does not have a precise extension because it is hard to judge whether an object belongs to the concept. Randomness is a deficiency of the law of probability and that fuzziness is a deficiency of the law of the excluded middle. Probability theory applies the random concept to generalized laws of probability. Fuzzy set theory applies the fuzzy property to the generalized law of the excluded middle, which is the law of membership from fuzziness (Hong and Vincent, 1995).

Probability reflects the internal relations and interactions of events under certain conditions. It could be very objective if a stable frequency is available from repeated experiments. Similarly, a stable frequency results from fuzzy statistical tests and can serve as the degree of membership in the objective sense. In many cases, the degree of membership can be determined by fuzzy statistical methods.

A random experiment has four basic requirements:

1. A sample space Ω that is formed by all related factors.
2. An event A that is a fixed and crisp subset of Ω.
3. A variable ω that is in Ω; once ω is determined, so are all the factors on their stated spaces.
4. A condition S that serve as restrictions on variable ω.

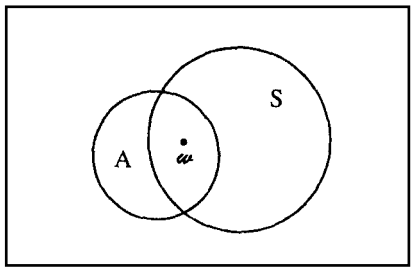

Figure 3.23 : A random experiment (*A* is fixed but ω varies)

The basic reason for randomness to exist is that the condition *S* is unable to restrict ω to a fixed point. Moreover, if $S \cap A \neq \Phi$ and $S \cap A^c \neq \Phi$ A, then $\omega \in S \cap A$ shows that the event *A* has occurred; otherwise it has not. That means *A* is a random event under the condition *S*. On random experiments, the following observations can be made:

1. The purpose of a random experiment is to study the uncertainty with certain or deterministic procedures.
2. A fundamental requirement of a random experiment is to clearly tell whether an event *A* has occurred or not.
3. A special characteristic of random experiment is that *A* is fixed, while ω is not.
4. After *n* times of repeated experiments, the frequency of *A* can be computed by Equation 3.13.

$$\text{Frequency of } A = \frac{\text{The number of trials when } \omega \in A}{n} \quad \text{[Eq. 3.13]}$$

It is well known that as *n* becomes very large, the above frequency tends to stabilize or converge to a fixed number. This number is called the probability of *A* under *S*.

A fuzzy statistical experiment has four basic requirements:

1. A universe *U*.
2. A fixed element $u_0 \in U$.
3. An adjustable crisp set A_* in *U* that is related to a fuzzy set.
4. A condition *S* that relates to all objective and psychological factors.

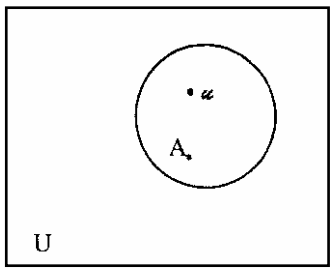

Figure 3.24 : A fuzzy statistical experiment (u_0 is fixed but A_* varies)

On the properties of fuzzy statistical experiments, the following observations can be made:

1. The purpose of fuzzy statistical experiments is to study uncertainties with certain or definite procedures.
2. A fundamental requirement of a fuzzy statistical experiment is to clearly tell whether $u_0 \in A_*$ or not.
3. A special characteristic of a fuzzy statistical experiment is that u_o is fixed, while A_* varies.
4. After collecting *n* sample observations from an experiment, the frequency of u_o in A_* can be computed by Equation 3.14.

$$\text{Frequency of } u_o \text{ in } A_* = \frac{\text{The number of observations of } u_0 \in A_*}{n} \qquad \text{[Eq. 3.14]}$$

As *n* increases, the frequency tends to converge to a fixed number; this number is called the degree of membership of u_o in A_*.

3.6.3 Interval analysis in arithmetic

In some complex systems that involve large quantities of data, it would be more reliable to give an interval estimate than just merely a point estimate. Take I_1 and I_2 for two interval numbers defined by ordered pairs of real numbers with lower and upper bounds.

$$I_1 = [a, b], \quad \text{where } a \leq b$$
$$I_2 = [c, d], \quad \text{where } c \leq d$$

When a = b and c = d, these interval numbers degenerate to a real number. A general arithmetic property is defined with the symbol $*$, where $* = \{ +, -, x, \div \}$. Operation between the two intervals result in another new interval. This interval calculation depends on the magnitudes and signs of the elements a, b, c, and d.

$$I_1 * I_2 = [a, b] * [c,d] \qquad \text{[Eq. 3.15]}$$

There are 6 possible combinations for elements of intersection and union as shown in Table 3.2.

Table 3.2 : Set operations on intervals (Dong and Shah, 1987)

Cases	Union	Intersection
a > d	[c, d] $\cup$ [a, b]	$\neg$
c > b	[a, b] $\cup$ [c, d]	$\neg$
a > c, b < d	[c, d]	[a, b]
c > a, d < b	[a, b]	[c, d]
a < c < b < d	[a, d]	[c, b]
c < a < d < b	[c, b]	[a, d]

Based on the information in Table 3.2, the four arithmetic operations associated with Equation 3.15 are given as follows:

$$[a,b] + [c,d] = [a + c, b + d] \quad \text{[Eq. 3.16]}$$

$$[a,b] - [c,d] = [a + c, b + d] \quad \text{[Eq. 3.17]}$$

$$[a,b] \bullet [c,d] = [\min(ac, ad, bc, bd), \max(ac, ad, bc, bd)] \quad \text{[Eq. 3.18]}$$

$$[a,b] / [c,d] = [a,b] \bullet \left[\frac{1}{d}, \frac{1}{c}\right], \text{ if } 0 \notin [c,d] \quad \text{[Eq. 3.19]}$$

Interval arithmetic follows properties of associativity and commutativity for both summations and products, but it does not follow the property of distributivity. Rather, intervals do follow a special subclass of distributivity known as subdistributivity. Assume that *I, J* and *K* are interval numbers;

Associativity:

$$I + (J + K) = (I + J) + K \quad \text{[Eq. 3.20]}$$

$$I \bullet (J \bullet K) = (I \bullet J) \bullet K \quad \text{[Eq. 3.21]}$$

Commutativity:

$$I + J = J + I \quad \text{[Eq. 3.22]}$$

$$I \bullet J = J \bullet I \quad \text{[Eq. 3.23]}$$

Subdistributivity:

$$I \bullet (J + K) \subset I \bullet J + I \bullet K \quad \text{[Eq. 3.24]}$$

Interval arithmetic can be illustrated by adding or multiplying two crisp numbers, then the result will be a crisp singleton. When adding or multiplying two intervals, an interval is expected as the result. In the simplest case, when multiplying two intervals containing only positive real numbers, it is easy conceptually to see that the interval comprising the solution is found by taking the product of the two lowest values from each of the intervals to form the solution's lower bound, and by taking the product of the two highest values from each of the intervals to form the solution's upper bound. Even though conceptually that an infinite number of combinations of products can be seen to be exist between these two intervals, only the end points of the intervals is needed to find the endpoints of the solution (Ross, 2004).

3.7 Monte Carlo Simulation

Monte Carlo analysis is a "brute force" solution to the problem of uncertainty analysis in environment models. It is conceptually very simple. Under this technique, probability density functions are assigned to each characteristic (variable or parameter) reflecting the uncertainty in that characteristic. Then, with "synthetic sampling", value are randomly chosen from the distribution for each term. These value are inserted into the model, and a prediction is calculated. After this is repeated a large number of times, a distribution of predicted value results, which reflects the combined uncertainties was developed.

As an example, Reckhow et al. (1980), Montgomery et al. (1980) and Lee (1980) used Monte Carlo simulation to study lake modelling errors for a simple phosphorus lake model. Distributions were defined (from existing data or expert judgment) for each uncertainty characteristics. Two of these distribution are presented in figures below, data are represented by histograms and a candidate probability model is shown as a smooth curve using normal distribution.

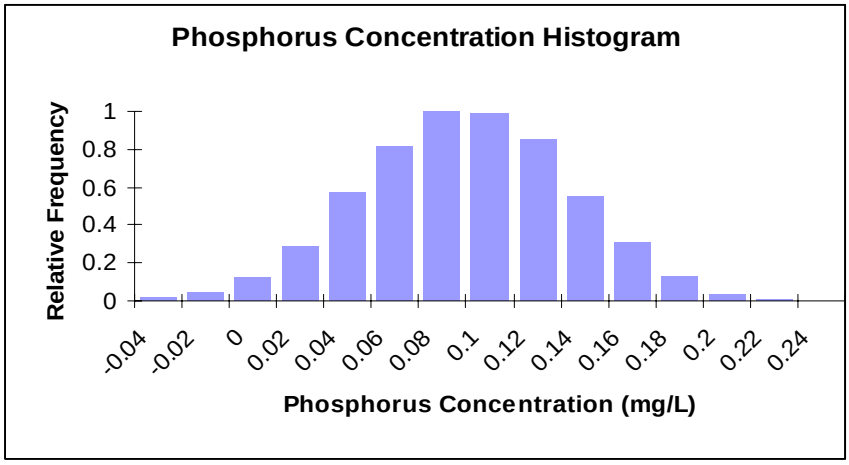

Figure 2: Output from Monte Carlo simulation (Histogram)

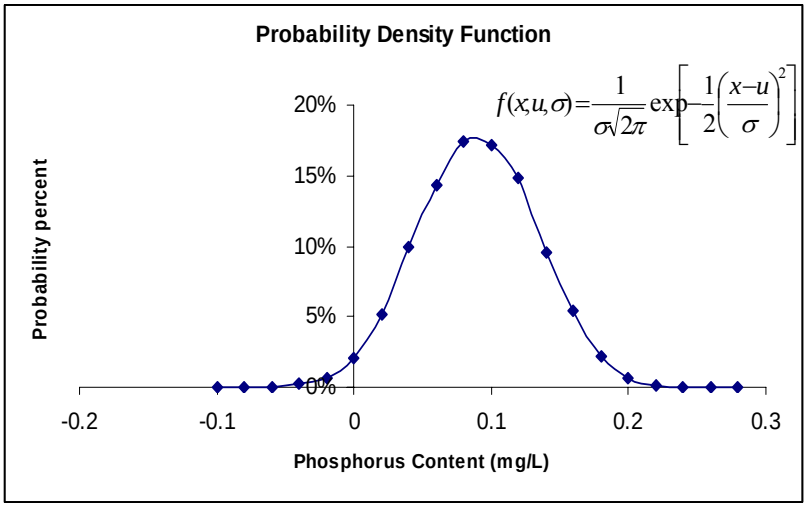

Figure 2: Output from Monte Carlo simulation (Probability Density Function)

CHAPTER 4

DATA ANALYSIS AND DISCUSSIONS

4.1 Data collection

There are four main type of data that need to be obtained in this study. The data were collected either by site investigations, sampling and testing, previous records or calculations. Some raw data will have to be analysed before it could be used. Later, the precipition, temperature and observed streamflow data will become the input to the IHACRES model to predict of streamflow for the catchment. The phophorus content and the modelled streamflow will be generated using fuzzy membership function with interval numbers operation for Vollenweider model.

4.2 Phosphorus content

Ten water samples were taken in each site visit from the ten stations within the catchment area. The water samples were brought back and tested at the laboratory to obtain the phosphorus content of the water samples. The same stations that were determined in the first visit were used for the second and third visits. There are some data that were unable to obtain in the second visit, which was caused by inaccessibility to the station area due to high water level that damaged the access roads.

Table 4.1 : Summary of phosphorus content in mg/l

Station	Location	21/12/06	10/7/07	21/2/07	Note
1	Sungai Ban Foo	0.245	0.193	0.094	along the inflowing river
2	Sungai Ban Foo	0.224	0.231	0.172	along the inflowing river
3	Sungai Ban Foo	0.131	-	0.053	along the inflowing river
4	Sungai Ban Foo	0.236	-	0.184	within wetland area
5	Sungai Ban Foo	0.195	-	0.059	within wetland area
6	Sungai Ban Foo	0.237	-	0.574	within wetland area
7	Sungai Layang	0.292	-	0.074	along the inflowing river (at V-notch)
8	Sungai Layang	0.255	-	0.060	along the inflowing river
9	Sungai Layang	0.392	0.240	0.622	along the inflowing river (at fish breeding pond)
10	Sungai Layang	0.113	0.211	0.053	along the inflowing river (near fish breeding pond)

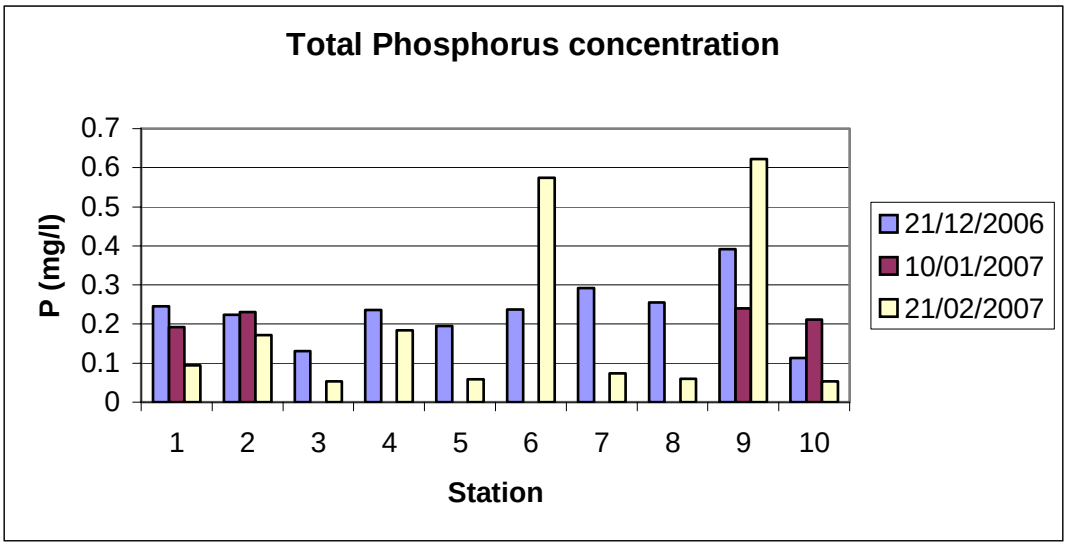

Figure 4.1 : Total phosphorus concentration from the three site visits

The total phoshorus concentration obtained from the three site visits were evaluated. The average phosphorus content was 0.214 mg/l. The highest phosphorus content recorded was 0.622 mg/l at Station 9 on the third visit. The lowest concentration which was 0.053 mg/l also obtained from the third visit at Station 10. This probably occurred because of the no rain period when the third visit was conducted. The flow observed in some area is small and in some area the flow might

be too small until there is little movement in the river, which can be considered as close to stagnant stage. The phosphorus concentration in the water will become high when the transportation of nutrients is slow.

4.3 Flow rates

Current meter was used to measure the velocity of the main rivers that flow in the catchment area. The flow rates of the rivers were determined using mid section method of the velocity - area method. The flow rates that has been calculated is used to determine the baseflow that will later be used in the IHACRES model during no rainfall periods. Some flow rates were unable to obtain in the second and third visits at the same stations as in the first visit because the stations could not be accessed.

Table 4.2 : Flow rate at Station 1 on 21/12/2006

Distance L (m)	**Depth y (m)**	**Velocity measured from surface depth 0.6y (m/s)**			**Average Velocity v (m/s)**	**Width B (m)**	**Area A = By (m^2)**	**Flow rate Q = Av (m^3/s)**
2.1	0.4	0.29	0.31	0.32	0.31	2.1	0.84	0.26
4.2	0.6	0.67	0.7	0.65	0.67	2.1	1.26	0.85
6.3	0.5	0.48	0.43	0.33	0.41	2.1	1.05	0.43
							Total =	1.54

Table 4.3 : Flow rates at Station 2 on 21/12/2006

Distance L (m)	**Depth y (m)**	**Velocity measured from surface depth 0.6y (m/s)**			**Average Velocity v (m/s)**	**Width B (m)**	**Area A = By (m^2)**	**Flow rate Q = Av (m^3/s)**
0.5	0.6	1.39	1.18	1.22	1.26	0.5	0.3	0.38
1.0	0.6	1.39	1.51	1.48	1.46	0.5	0.3	0.44
1.5	0.6	1.32	1.25	1.31	1.29	0.5	0.3	0.39
							Total =	1.21

Table 4.4 : Flow rate at Station 7 on 21/12/2006

Distance L (m)	Depth y (m)	Velocity measured from surface depth 0.6y (m/s)			Average Velocity v (m/s)	Width B (m)	Area A = By (m^2)	Flow rate Q = Av (m^3/s)
0.75	0.6	0.24	0.23	0.24	0.24	0.75	0.45	0.11
							Total =	0.11

Table 4.5 : Flow rate at Station 8 on 21/12/2006

Distance L (m)	Depth y (m)	Velocity measured from surface depth 0.6y (m/s)			Average Velocity v (m/s)	Width B (m)	Area A = By (m^2)	Flow rate Q = Av (m^3/s)
0.75	0.55	0.18	0.19	0.20	0.19	0.75	0.41	0.08
							Total =	0.08

Table 4.6 : Flow rate at Station 2 on 10/01/2007

Distance L (m)	Depth y (m)	Velocity measured from surface depth 0.6y (m/s)			Average Velocity v (m/s)	Width B (m)	Area A = By (m^2)	Flow rate Q = Av (m^3/s)
0.5	0.7	0.28	0.27	0.29	0.28	0.5	0.35	0.10
1.0	0.7	0.25	0.22	0.20	0.22	0.5	0.35	0.08
1.5	0.7	0.19	0.18	0.25	0.21	0.5	0.35	0.07
							Total =	0.25

Table 4.7 : Flow rate at Station 1 on 21/02/2007

Distance L (m)	Depth y (m)	Velocity measured from surface depth 0.6y (m/s)			Average Velocity v (m/s)	Width B (m)	Area A = By (m^2)	Flow rate Q = Av (m^3/s)
2.5	0.8	0.01	0.01	0.01	0.01	2.5	2.00	0.02
5.0	0.9	0.01	0.01	0.01	0.01	2.5	2.25	0.02
7.5	0.8	0.01	0.01	0.01	0.01	2.5	2.00	0.02
							Total =	0.06

Table 4.8 : Flow rate at Station 2 on 21/02/2007

Distance L (m)	Depth y (m)	Velocity measured from surface depth 0.6y (m/s)			Average Velocity v (m/s)	Width B (m)	Area A=By (m2)	Flow rate Q=Av (m3/s)
0.5	1.0	0.02	0.01	0.02	0.02	0.5	0.5	0.01
1.0	1.0	0.01	0.02	0.02	0.02	0.5	0.5	0.01
1.5	1.0	0.02	0.02	0.01	0.02	0.5	0.5	0.01
							Total =	0.03

Table 4.9 : Summary of flow rate in m^3/s

Station	Location	21/12/2006	10/01/2007	21/02/2007
1	Sungai Ban Foo	1.54	0.25	0.06
2	Sungai Ban Foo	1.21	-	0.03
7	Sungai Layang	0.11	-	-
8	Sungai Layang	0.08	-	-

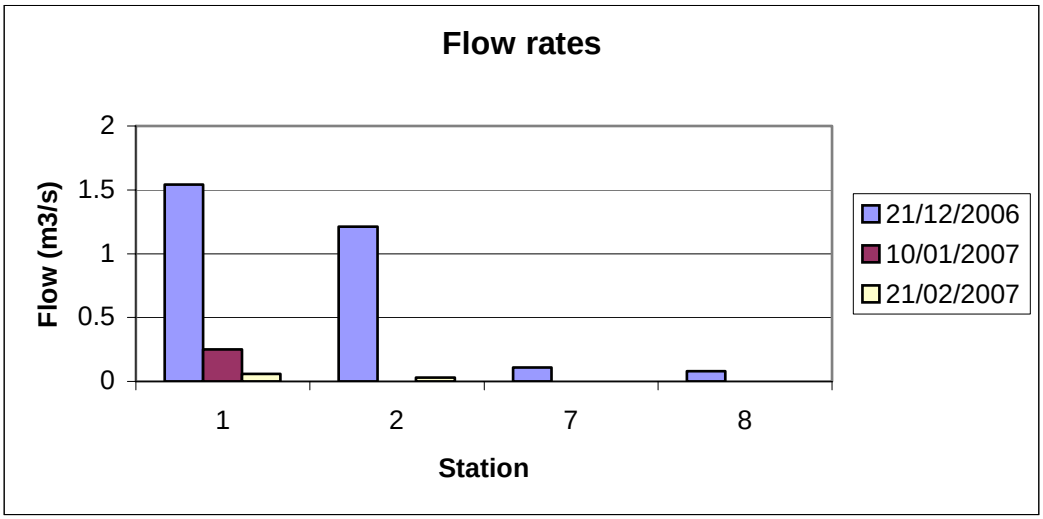

Figure 4.2 : Flow rates from the three site visits

The highest value of streamflow 1.54 m^3/s was recorded during the first visit and the lowest value 0.03 m^3/s was obtained from the third visit. The first visit was conducted during rainy season, while the third visit conducted during no rainfall period. There was evident difference between the streamflow measured. During the

first visit, the flow of the river is observed to be high. Meanwhile, the observation result from the third visit was that there was only small flow in the river.

4.4 Temperature

Daily temperature data were obtained as an input for the IHACRES model. The data was obtain from the Malaysian Meteorological Department. The station for the temperature measurement is located at Senai with the station number 48679. It is 37.8 m above mean sea level and situated in the coordinates of latitudes 1^{o} 38' N and longitudes 103^{o} 40' E.

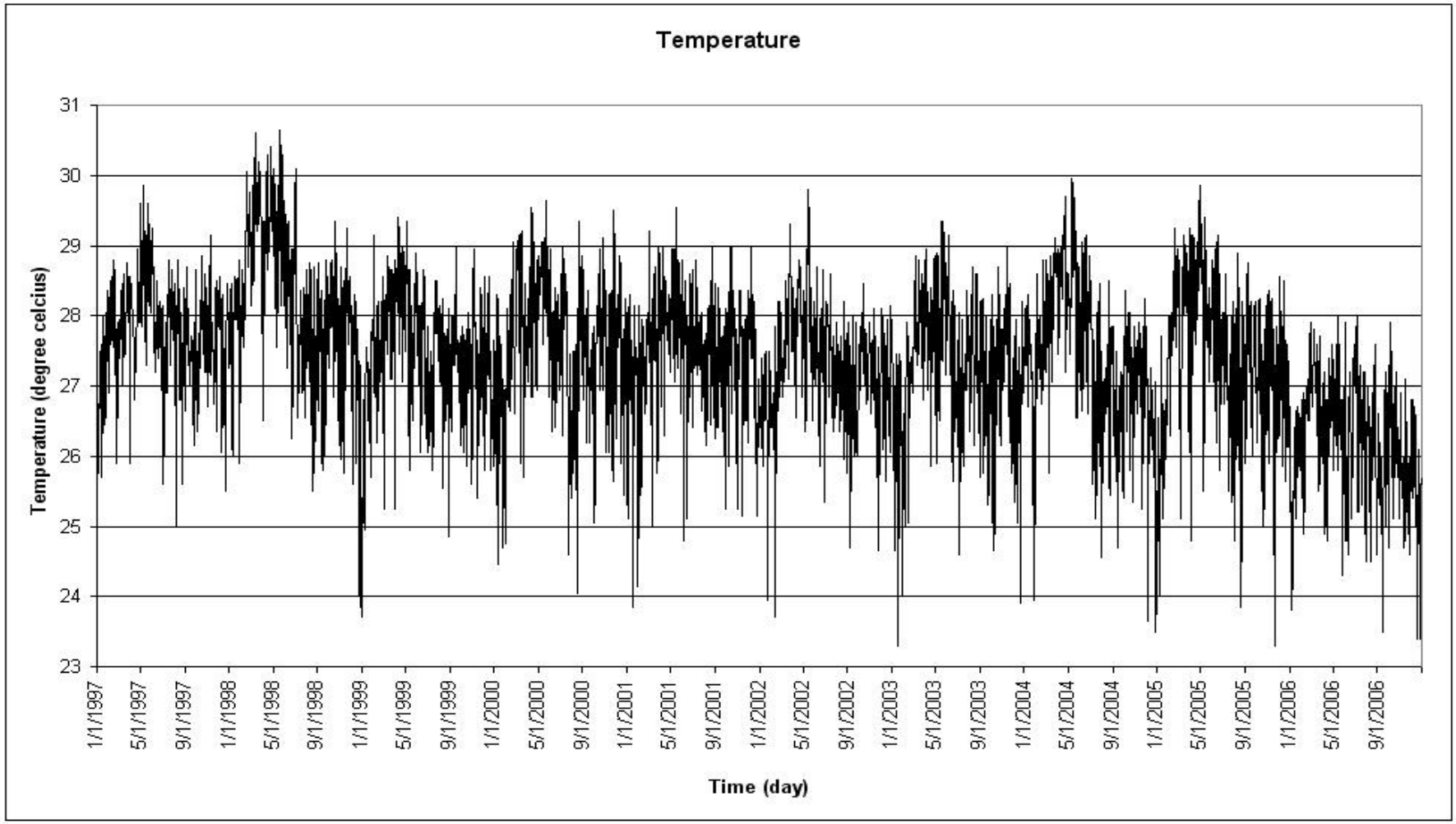

Figure 4.3 : Graph of temperature

The record of temperature data was taken for a period of ten years which is from 1 January 1997 until 31 December 2006. The highest temperature value was 30.65 degree celcius on 21/5/1998 and the lowest temperature value was 23.3 degree celcius on 19/01/2003 and 22/11/2005. Assumption made here was that the temperature recorded as Senai will represent the temperature at site because the effect of temperature is more global. Therefore, as long as the two location were not very far away from each other, the effect of temperature change is considered as minimum and negligible.

4.5 Precipitation

Rainfall data were obtained from the Department of Irrigation and Drainage Malaysia for the Station 1539001, Loji air Sungai Layang. The period of rainfall were also ten years that is from 1997 to 2006. There were some missing data in the ten years periods and therefore the data must be analysed first to ensure its continuity because the IHACRES model cannot recognize broken data values and may result in error. The missing data were filled with data from other nearby stations or the period that is nearest to the average distributions. Since the refilled data may not represent the actual condition of precipitation in the catchment area, the calibration period for the IHACRES model were not chosen in the period of missing data.

The rainfall data will be shown in Figure 4.4. The highest rainfall value is 241 mm which was recorded in 28/12/2001 and the lowest value is zero which was the occurrence of no rainfall period. It can be observed that the peak which represent high rainfall will normally occur at the end of the year which is during the rainy season.

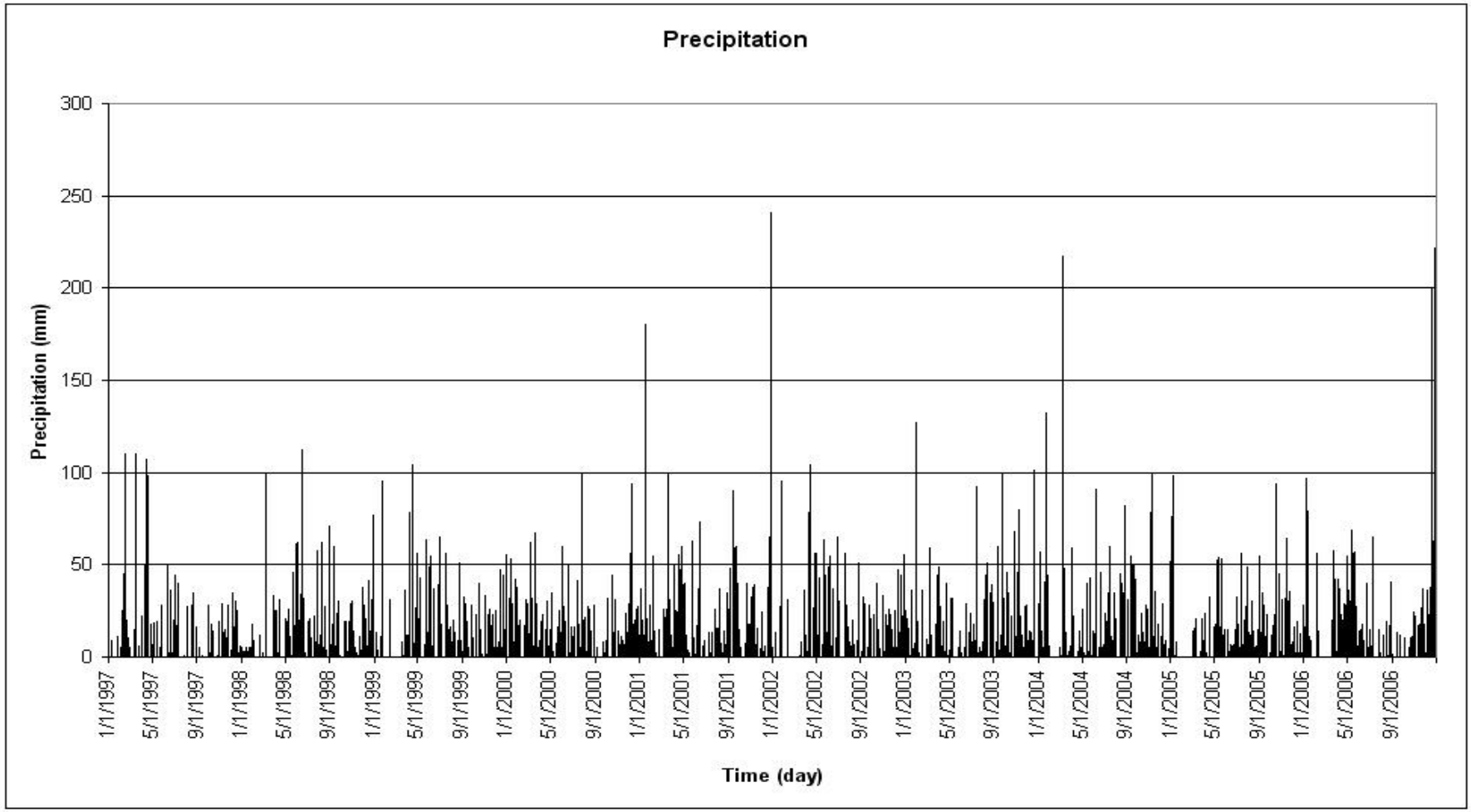

Figure 4.4 : Daily rainfall of Layang (Station 1539001)

4.6 Evaporation

Evaporation data is used for runoff analysis of the catchment, which is also regard as the observed streamflow. Daily evaporation data for Station 1539301 were obtained from the Department of Irrigation and Drainage Malaysia with the same period as the rainfall. There also exist some missing data and the missing data were filled with data from other nearby stations or the period that is nearest to the average distributions.

The evaporation data will be shown in Figure 4.5. The highest evaporation is 12 mm which was recorded in 9/1/2003 and the lowest is zero which indicates that no evaporation occurs during the period.

4.7 Infiltration

Infiltration data will have to be calculated for the use in the storage equation in runoff analysis later. The Horton model is used for the calculation of infiltration values. The parameter used are based on Table 14.4 from the MASMA manual. The soil at the research area can be classified as loam soil which consists of sand, clay and silt in approximately equal proportions (Faradilah, 2006).

$$\text{Infiltration Rate,} \quad F = f_c + (f_o - f_c)e^{-Kt} \qquad \text{[Eq. 4.1]}$$

where f_o = Initial infiltration rate
= 75 mm / hr
f_c = Final infiltration rate
= 5.65 mm / hr
t = time (hr)
K = Coefficient (4 hr)

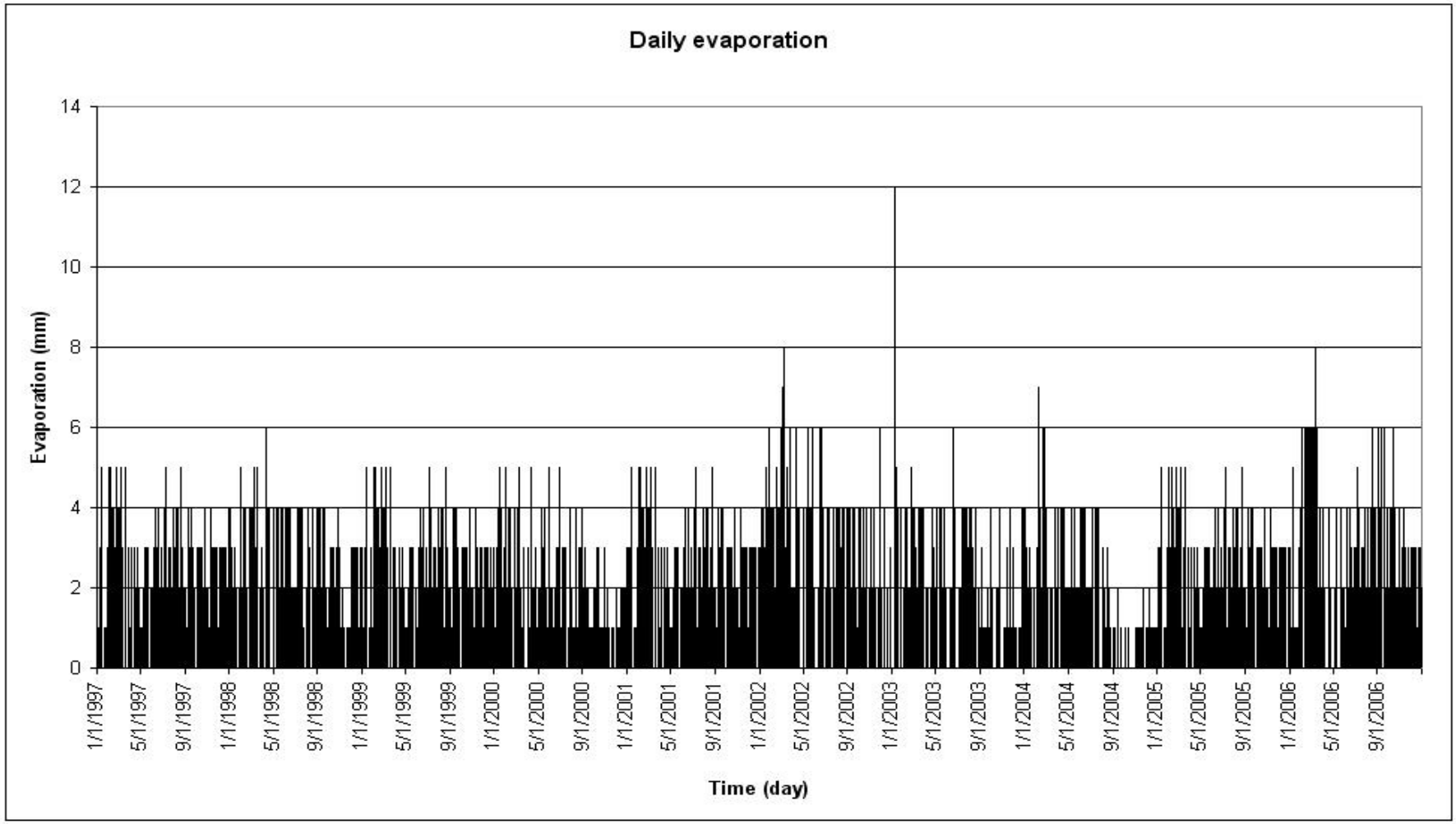

Figure 4.5 : Daily evaporation of Layang (Station 1539301)

The rainfall durations per year are calculated from the average total rainfall per year by assuming that 1 mm of rainfall equals to 2 minutes of time. The intensity of the rainfall is assumed to be constant within the rainfall duration. The rainfall data are recorded daily, therefore the total hour rainfall for the period should be computed (Norliza, 2005).

For the calculation, every annual total rainfall will be converted to determine the rainfall duration per year in hour unit. Then, the Horton model is used to calculate the infiltration rate. The infiltration rate is later multiplied by rainfall duration to determine the infiltration per year. Then, the infiltration value is divided with the total days per year to determine the average daily infiltration.

Example calculation:

Total rainfall in the year 1997 = 1982.2 mm

Assuming 1 mm rainfall duration = 2 minutes

Rainfall duration in hour = Total rainfall × 2 mins × 1 hr / 60 mins

= 1982.2 × 1/30 hr

= 66.1 hour

Infiltration rate, $F = f_c + (f_o - f_c)e^{-Kt}$

$= 5.65 + (69.35)e^{-4(66.1)}$

= 5.65 mm / hour

Infiltration per year = Rainfall duration × Infiltration rate

= 66.1 × 5.65

= 373.5 mm

Average daily infiltration = Total infiltration / Total days per year

= 373.5 / 365

= 1.023 mm

Table 4.10 : Average daily infiltration

Year	Total rainfall per year (mm)	Rainfall duration per year (hour)	Infiltration rate (mm/hr)	Total infiltration per year (mm)	Average daily infiltration (mm)
1997	1982.2	66.1	5.65	373.5	1.023
1998	2345.0	78.2	5.65	441.8	1.210
1999	2312.6	77.1	5.65	435.6	1.193
2000	2330.0	77.7	5.65	439.0	1.203
2001	3134.0	104.5	5.65	590.4	1.618
2002	2312.6	77.1	5.65	435.6	1.193
2003	2553.0	85.1	5.65	480.8	1.317
2004	2670.5	89.0	5.65	502.9	1.378
2005	2322.0	77.4	5.65	437.3	1.198
2006	2946.5	98.2	5.65	554.8	1.520

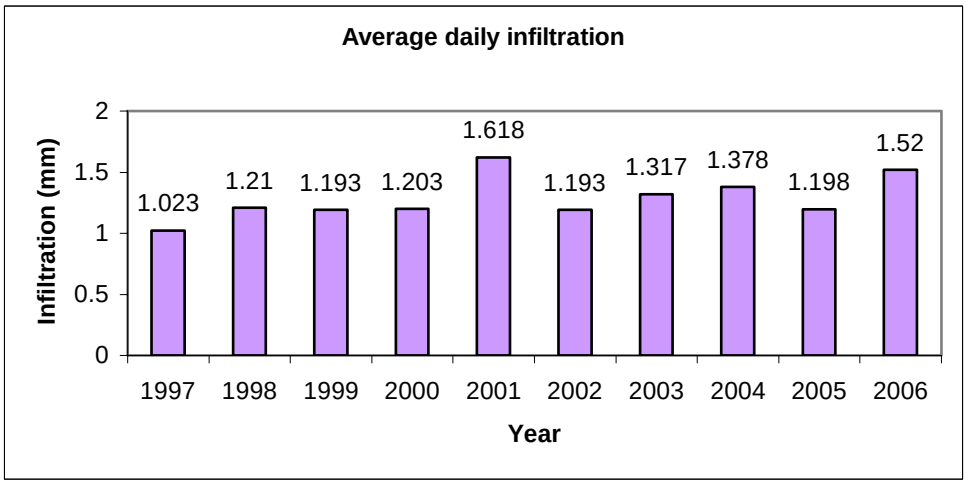

Figure 4.6 : Average daily infiltration

The highest average daily infiltration is in the year 2001 with the value of 1.618 mm. The lowest value for average daily infiltration is 1.023 mm in 1997.

4.8 Streamflow analysis

4.8.1 Observed streamflow

As a requirement for input in IHACRES, the observed streamflow data is computed by using storage equation. These total rainfall are then deducted with the total evaporation and annual infiltration. At the end of the calculation, the unit are converted to liter per second for the use of the input in IHACRES model.

Surface Runoff = Total rainfall - Total evaporation - Total infiltration

The daily rainfall data for the period of 1997 until 2006 will be multiplied with the watershed area of 50.5 km^2 to determine the inflow rate. The average daily evaporation data are multiplied with the reservoir surface area of 30.5 km^2. This area is considered to be saturated where all the water that did not absorbed into the ground will flow into the reservoir. The evaporation is considered occurring within the reservoir only. For infiltration data, the average daily infiltration is multiplied with the watershed area that had been subtracted from the reservoir area. This is because the reservoir is considered saturated with no infiltration process (Faradilah, 2006).

Example calculation for 09/01/2007:

Daily rainfall	=	9.0 mm
Watershed area	=	50.5 km^2
	=	50.5×10^6 m^2
Volume of rainfall per day	=	$(9.0 \times 10^{-3}) \times (50.5 \times 10^6)$
	=	454500 m^3/ day

Daily evaporation = 1.0 mm

Reservoir surface area = $30.5\ km^2$

= $30.5 \times 10^6\ m^2$

Volume of evaporation per day = $(1.0 \times 10^{-3}) \times (30.5 \times 10^6)$

= $30500\ m^3$ / day

Average daily infiltration = 1.023 mm

Watershed area = $50.5 \times 10^6\ m^2$

Reservoir surface area = $30.5 \times 10^6\ m^2$

Infiltration area = Watershed area - Reservoir surface area

= $(50.5 \times 10^6\ m^2) - (30.5 \times 10^6\ m^2)$

= $20 \times 10^6\ m^2$

Volume of infiltration per day = Daily infiltration × Infiltration area

= $(1.023 \times 10^{-3}) \times (20 \times 10^6)$

= $20460\ m^3$/ day

Volume of rainfall = $454500\ m^3$/ day

Volume of evaporation = $30500\ m^3$ / day

Volume of infiltration = $20460\ m^3$/ day

Total surface runoff = 454500 - 30500 - 20460

= $403540\ m^3$/ day

= $4.67\ m^3$ / s

= 4670 l / s

4.8.2 Modelled streamflow

After all the input required were prepared, the IHACRES modelling can be initiated. All the three inputs which are rainfall, temperature and observed streamflow are loaded into the software. The calibration period is defined before the calibration process begin. Period where high peaks occur are avoided when choosing the calibration period because the high peak phenomenas are not a usual occurrence and therefore they do not represent the catchment as a whole. After the calibration period has been set, then the model is calibrated to obtain the best parameters that can describe the catchment.

Table 4.11 : Non linear model module calibration result

mass balance term (c)	0.012508
drying rate at reference temperature (tw)	4.000000
temperature dependence of drying rate (f)	0.000000
reference temperature (tref)	26.00000
moisture threshold for producing flow (l)	0.000000
power on soil moisture (p)	0.200000

Table 4.12 : Linear model module calibration result

Recession rate 1 ($\alpha^{(s)}$)	-0.000
Peak response 1 ($\beta^{(s)}$)	1.000
Time constant 1 ($\tau^{(s)}$)	0.113
Volume proportion 1 ($v^{(s)}$)	1.000

The simulation process begin after the calibration step is completed. The hydrograph that is generated from the simulation shows graphical representation of the simulation result as shown in Figure 4.7. The values can be obtained from the simulation summary. The overall simulation result performance can be seen at the

statistic summary table. From the statistic summary table, the two main performance statistics that are referred to are the bias and R squared. R squared is also known as the efficiency and the value should be close to unity, which is 1. On the other hand, the bias should be as close to zero as possible.

$$\text{Bias} = \frac{\sum (Q_o - Q_m)}{n} \qquad \text{[Eq. 4.2]}$$

$$\text{R squared} = 1 - \frac{\sum (Q_o - Q_m)^2}{\sum (Q_o - \overline{Q_o})^2} \qquad \text{[Eq. 4.3]}$$

where Q_o is the observed streamflow value

Q_m is the modelled streamflow value

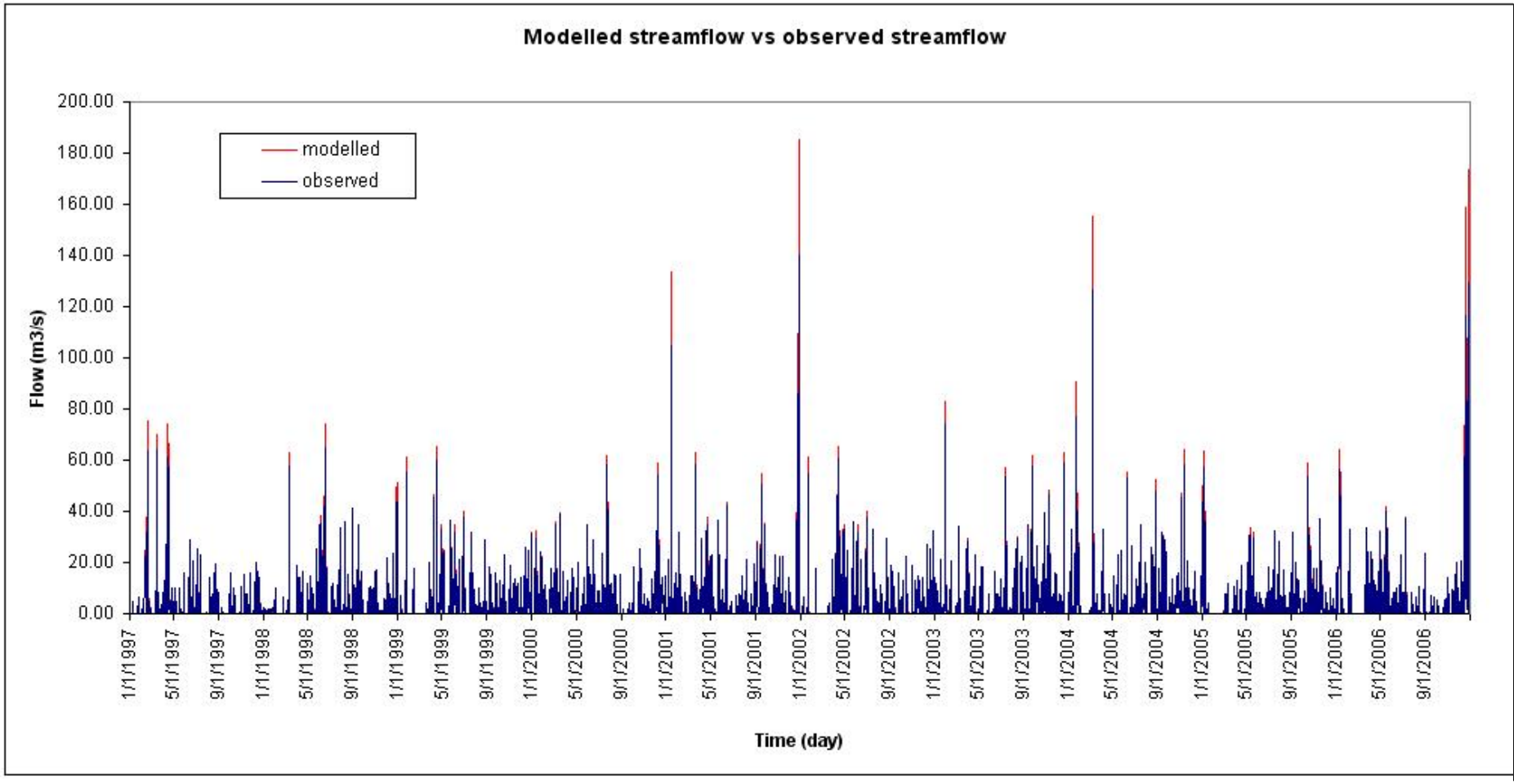

Figure 4.7 : Graph of modelled streamflow vs observed streamflow

Table 4.13 : Statistic summary for the calibration period

Period	Bias (mm/d)	R squared
1997	-0.0076	0.9764
1998	0.0171	0.9866
1999	0.0574	0.9925
2000	0.2839	0.9916
2001	-0.2840	0.9457
2002	0.2382	0.9918
2003	0.2284	0.9918
2004	0.0420	0.9733
2005	0.0389	0.9896
2006	-0.5546	0.9208

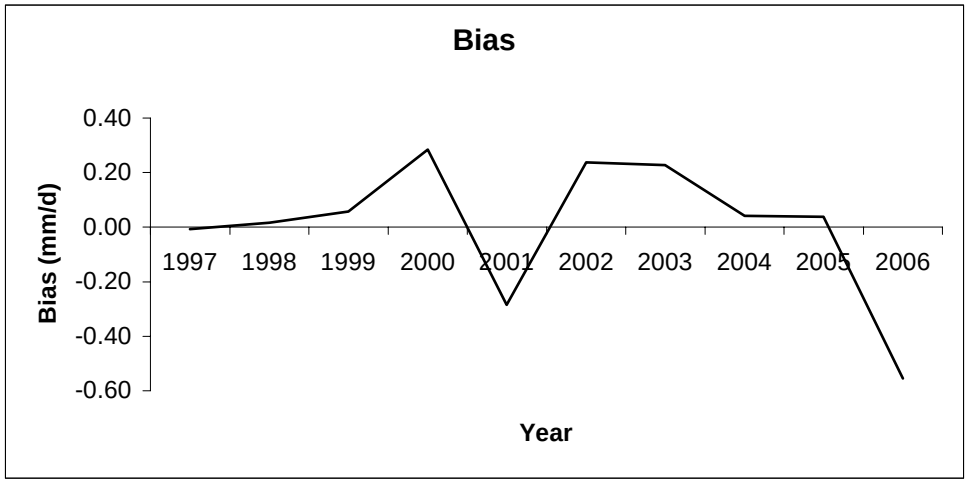

Figure 4.8 : Average daily bias for the simulation period

The largest bias is -0.5546 mm/day and the smallest bias is -0.0076 mm/day. These values are close to zero and therefore it is acceptable. The high bias occur most probably when there exist some high peaks in the hydrograph of the observed streamflow. The model was not calibrated according to the performance of high peaks, so there might happen some errors in predicting the high peaks and this result in the bias.

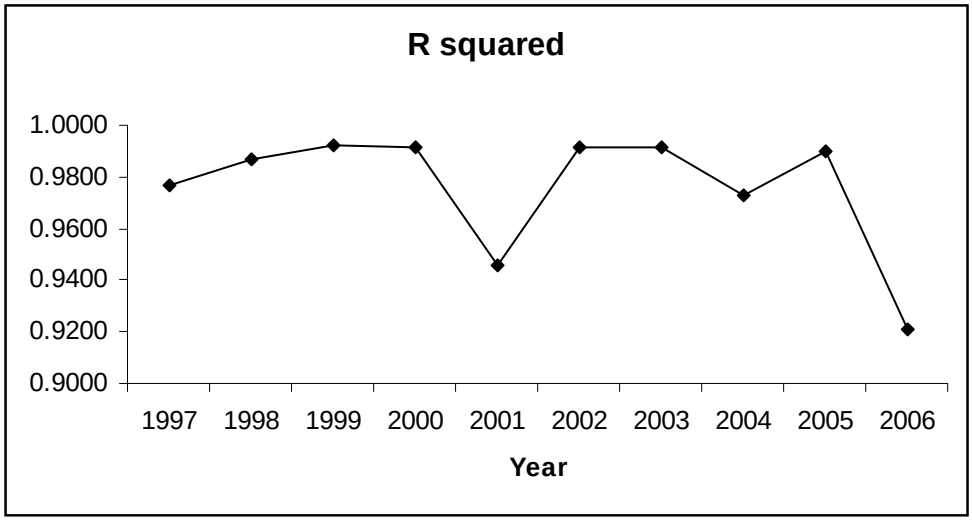

Figure 4.9 : R squared value for the simulation period

The highest R squared value is 0.9925 while the lowest is 0.9208. These values are considered as quite high as the lowest value is still above 0.90 Both can be considered near to 1. This indicates that the model is able to perform quite well.

4.9 Fuzzy membership functions

The membership functions for phosphorus and hydraulic loading could be obtained after all the data were prepared. The data were grouped to determine the frequency in each group. The relative frequency is then calculated from dividing the frequency in each interval by the highest frequency.

The annual hydraulic loading as shown in Table 4.14 and Table 4.15 was calculated after the modelled streamflow data were obtained. The highest value for annual

hydraulic loading was 1897.53 m/yr from the year 2001 and lowest value was 1149.81 m/yr from the year 1997. The average hydraulic loading was 1452.25 m/yr.

Table 4.14 : Hydraulic loading in unit m/yr for 1997-2001

	1997	**1998**	**1999**	**2000**	**2001**
January	8.13	31.06	104.19	169.57	298.98
February	258.67	24.23	17.97	98.82	59.46
March	105.48	104.22	31.48	148.38	170.37
April	312.25	61.85	228.04	75.85	239.21
May	42.47	94.60	146.91	76.73	127.36
June	81.38	243.08	200.40	134.53	85.94
July	60.57	99.91	114.52	159.12	42.59
August	71.17	139.71	63.47	62.49	85.94
September	2.18	124.98	80.99	6.62	255.45
October	54.97	90.88	55.69	82.68	63.08
November	57.79	39.63	102.04	61.25	131.13
December	94.77	272.40	173.04	218.37	338.02
Total	1149.81	1326.54	1318.74	1294.42	1897.53

Table 4.15 : Hydraulic loading in unit m/yr for 2002-2006

	2002	**2003**	**2004**	**2005**	**2006**
January	104.14	200.60	265.15	179.44	276.03
February	17.97	72.61	3.23	0.00	44.75
March	31.48	88.63	231.45	45.39	80.65
April	228.04	137.35	77.85	42.54	142.49
May	146.91	63.41	72.12	217.00	244.83
June	200.40	36.18	106.08	57.24	86.89
July	114.52	104.26	143.09	148.61	79.31
August	63.47	177.40	163.38	65.09	61.93
September	80.99	168.24	147.22	157.25	14.86
October	55.69	162.45	113.40	183.98	30.79
November	102.04	126.74	184.37	159.21	77.15
December	173.04	119.66	72.19	56.28	727.95
Total	1318.69	1457.53	1579.53	1312.03	1867.64

Table 4.16 : Frequency of phosphorus content membership

Order	Grouping (mg/l)	Frequency	Relative frequency
1	0.00	0	0.00
2	0.01 - 0.05	0	0.00
3	0.06 - 0.10	6	0.86
4	0.11 - 0.15	2	0.29
5	0.16 - 0.20	4	0.57
6	0.21 - 0.25	7	1.00
7	0.26 - 0.30	2	0.29
8	0.31 - 0.35	0	0.00
9	0.36 - 0.40	1	0.14
10	0.41 - 0.45	0	0.00
11	0.46 - 0.50	0	0.00
12	0.51 - 0.55	0	0.00
13	0.56 - 0.60	1	0.14
14	0.61 - 0.65	1	0.14
15	0.66 - 0.70	0	0.00
16	0.71 - 0.75	0	0.00

Table 4.17 : Frequency of hydraulic loading membership

Order	Grouping (m/yr)	Frequency	Relative frequency
1	0	0	0.00
2	1 - 50	0	0.00
3	51 - 100	0	0.00
4	101 - 150	0	0.00
5	151 - 200	0	0.00
6	201 - 250	0	0.00
7	251 - 300	0	0.00
8	301 - 350	0	0.00
9	351 - 400	0	0.00
10	401 - 450	0	0.00
11	451 - 500	0	0.00
12	501 - 550	0	0.00
13	551 - 600	0	0.00
14	601 - 650	0	0.00
15	651 - 700	0	0.00
16	701 - 750	0	0.00
17	751 - 800	0	0.00
18	801 - 850	0	0.00
19	851 - 900	0	0.00
20	901 - 950	0	0.00
21	951 - 1000	0	0.00
22	1001 - 1050	0	0.00
23	1051 - 1100	0	0.00
24	1101 - 1150	1	0.25
25	1151 - 1200	0	0.00
26	1201 - 1250	0	0.00
27	1251 - 1300	1	0.25
28	1301 - 1350	4	1.00
29	1351 - 1400	0	0.00
30	1401 - 1450	0	0.00
31	1451 - 1500	1	0.25
32	1501 - 1550	0	0.00
33	1551 - 1600	1	0.25
34	1601 - 1650	0	0.00
35	1651 - 1700	0	0.00
36	1701 - 1750	0	0.00
37	1751 - 1800	0	0.00
38	1801 - 1850	0	0.00
39	1851 - 1900	2	0.50
40	1901 - 1950	0	0.00

After the relative frequency for the phosphorus content and hydraulic loading were calculated, the histogram of the membership function for both the data can be drawn. The histograms are shown in Figure 4.10 and Figure 4.11.

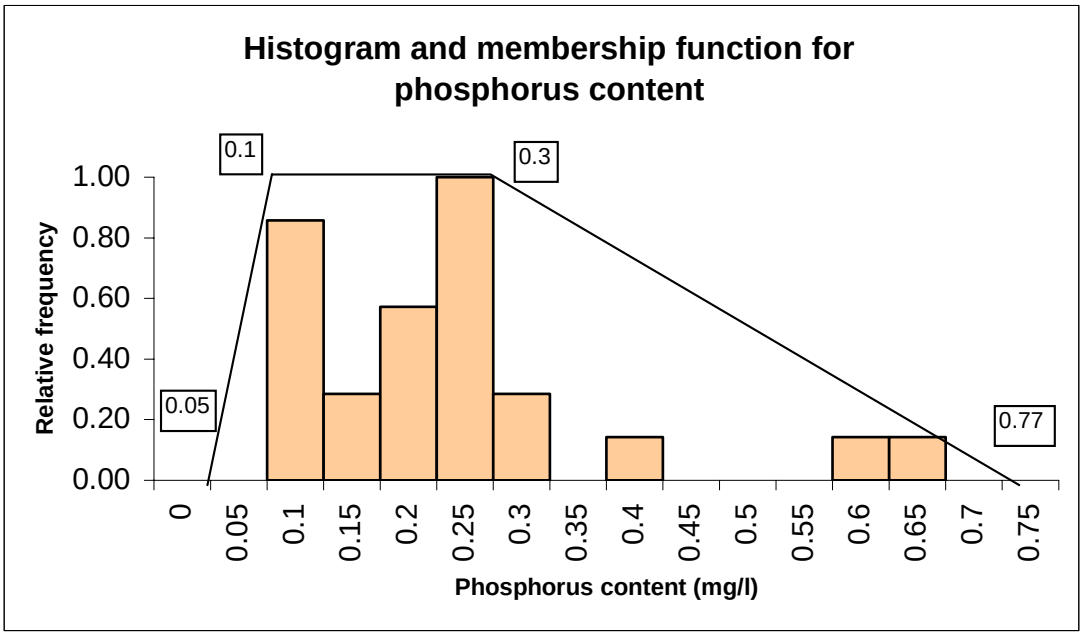

Figure 4.10 : Histogram and membership function for phosphorus content

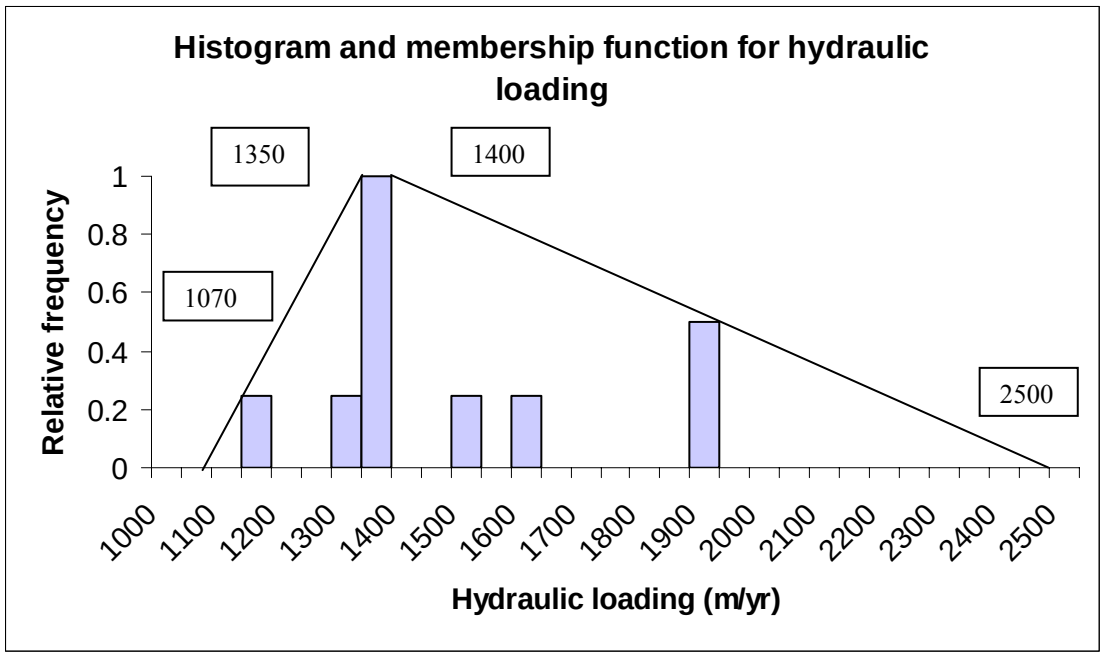

Figure 4.11 : Histogram and membership function for hydraulic loading

The histograms show that both of the data are represented by the trapezoid membership function. The support and core of the membership functions are determined after membership function were drawn. From Figure 4.12, the boundaries for phosphorus content membership function are 0.05mg/l, 0.1mg/l, 0.3mg/l and 0.77 mg/l. From Figure 4.13, the boundaries for hydraulic loading membership function are 1070m/yr, 1350m/yr, 1400m/yr and 2500 m/yr.

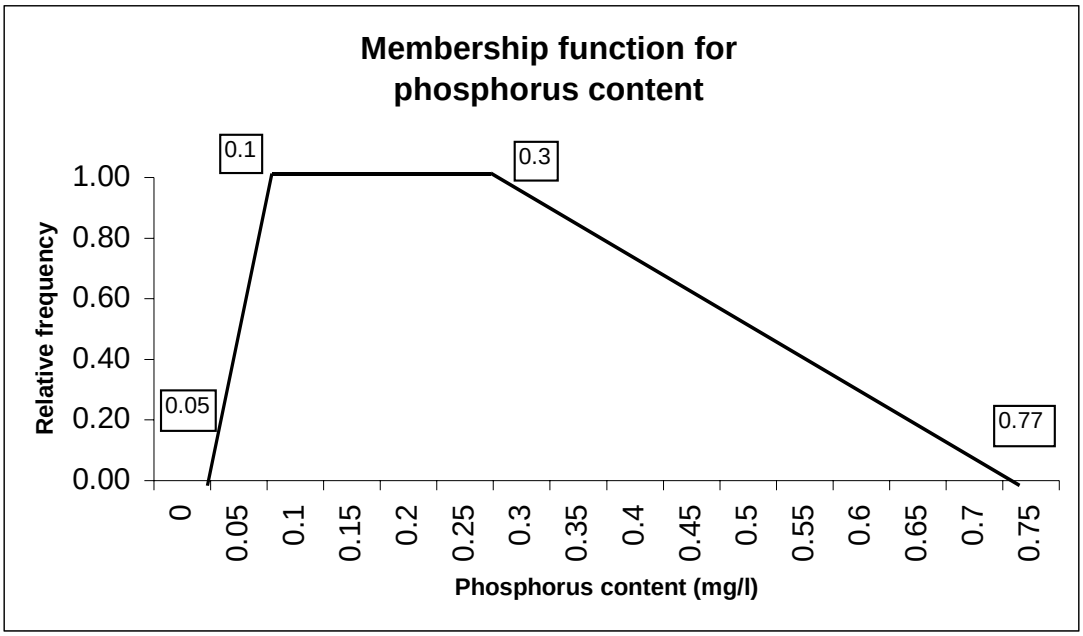

Figure 4.12 : Membership function for phosphorus content

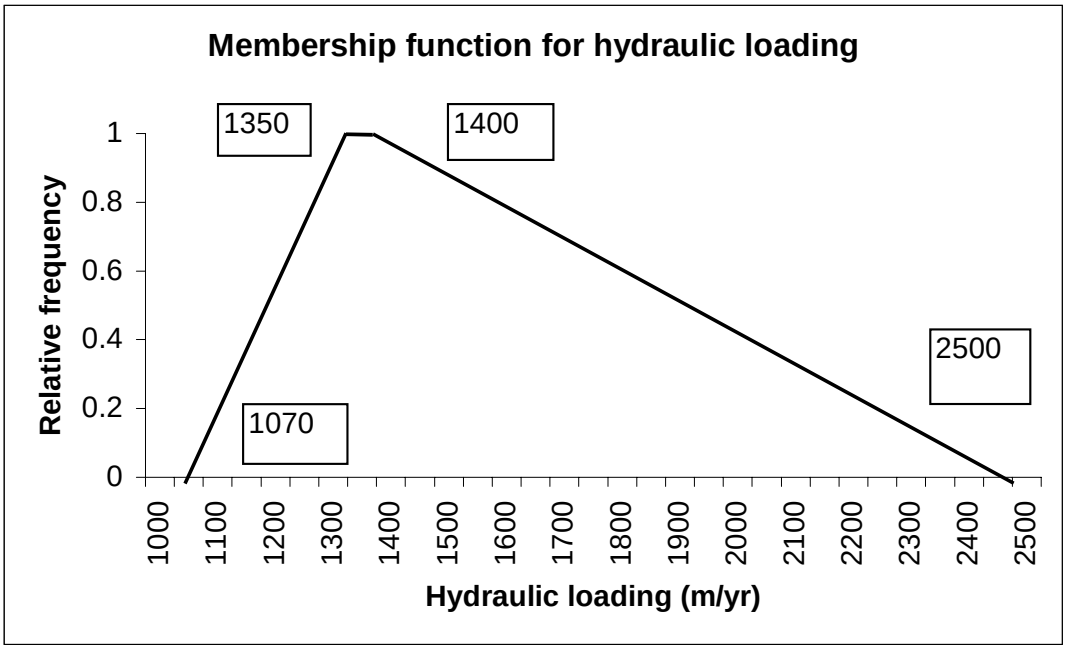

Figure 4.13 : Membership function for hydraulic loading

From the Vollenweider model as in Equation 3.1, P is represented by the membership function for phosphorus content and q_s is represented by the membership function for hydraulic loading. The T_w value used is 0.86 yr (Supiah, 1997). The membership function for the phosphorus loading are determined by using arithmetic operation as in Equation 3.18. The operation is done to find the core and support of the phosphorus loading membership function. [a,b] represent the interval number in membership function for phosphorus content, while [c,d] represent the interval number membership function for hydraulic loading. The membership function for phosphorus loading is shown in Figure 4.14.

At the core,

$$
\begin{aligned}
[a,b] \bullet [c,d] &= [0.1, 0.3] \bullet [1350, 1400] \\
&= [\min (135, 140, 405, 420), \max (135, 140, 405, 420)] \\
&= [135, 420]
\end{aligned}
$$

At the support,

$$
\begin{aligned}
[a,b] \bullet [c,d] &= [0.05, 0.77] \bullet [1070, 2500] \\
&= [\min (53.5, 125, 823.9, 1925), \max (53.5, 125, 823.9, 1295)] \\
&= [53.5, 1925]
\end{aligned}
$$

Example of calculation:

At the support,

$$
\begin{aligned}
Lp &= P \,.\, qs \,.\, (1 + \sqrt{T_w}) \\
&= 53.5 \,.\, (1 + \sqrt{T_w}) \\
&= 53.5 \,.\, (1 + \sqrt{0.86}) \\
&= 100 \text{ mg/m}^2\text{/yr} \\
&= 0.1 \text{ g/m}^2\text{/yr}
\end{aligned}
$$

From Figure 4.14, the range of phosphorus loadings estimated were 0.1g/m^2/yr to 3.71 g/m^2/yr. This result was the prediction or estimation used to describe the phosphorus loadings range in the Layang reservoir. It could be said that the phosphorus loadings that most likely to happen were 0.26 g/m^2/yr to 0.81 g/m^2/yr because of the degree of membership function is at 1. The lower the degree of the membership function, the less likely the loading is likely to happen. On the other hand, the closer the degree of the membership function to 1, the more likely for the loading to happen.

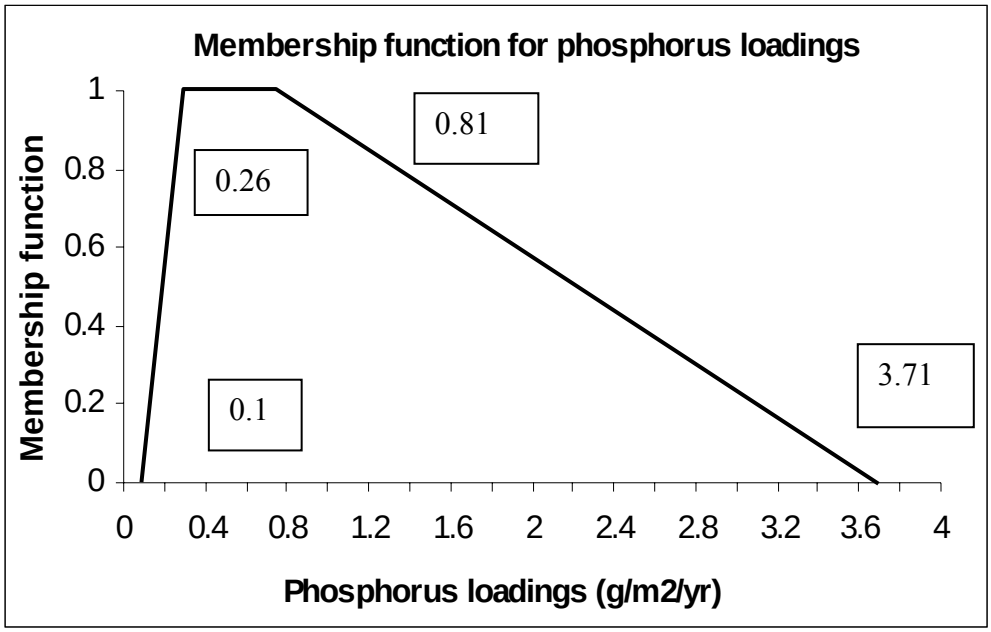

Figure 4.14 : Membership function for phosphorus loadings in g/m^2/yr

The average phosphorus content was 0.214 mg/l and average hydraulic loading was 1452.25 m/yr. The average phosphorus loading calculated was 0.6g/m^2/yr. From Figure 4.14, the degree of membership for 0.6 g/m^2/yr is 1, which means it is most likely to happen. 0.6 g/m^2/yr is also within the estimated most likely range of 0.26g/m^2/yr to 0.81 g/m^2/yr.

The overall phosphorus loadings estimated was ranged from 3.09 ton/yr to 111.31 ton/yr, with the most likely to happen condition ranging from 7.81 ton/yr to 24.28 ton/yr as shown in Figure 4.15.

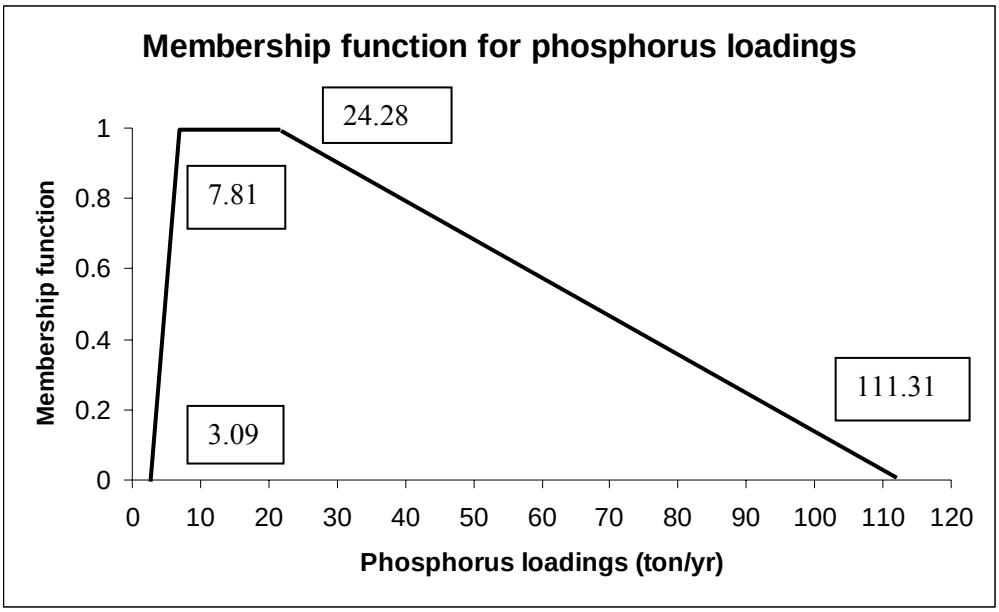

Figure 4.15 : Membership function for phosphorus loadings in ton/yr

The average phosphorus loading calculated was 17.97 ton/yr. From Figure 4.15, the degree of membership for 17.97 ton/yr is 1, which means it is most likely to happen. 17.97 ton/yr is also within the estimated most likely range of 7.81 ton/yr to 24.28 ton/yr.

4.10 Monte Carlo Simulation

Figure 4.16 and Figure 4.17 showed the histogram and normal distribution of phosphorus and hydraulic frequency.

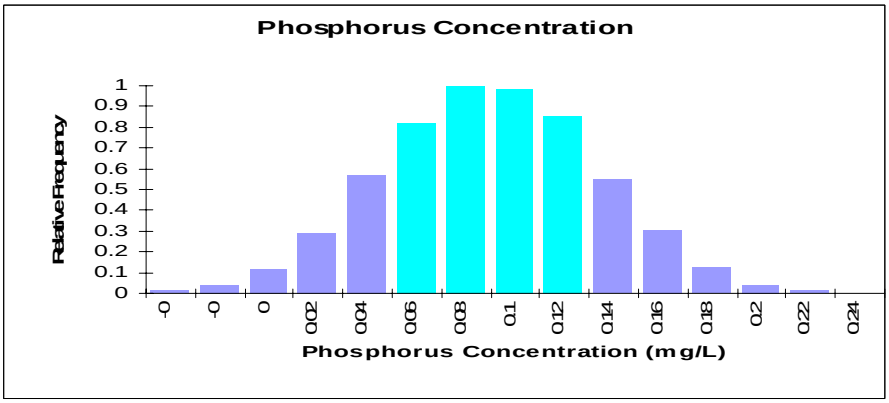

Figure 4.16: Normal distribution of phosphorus concentration (mg/l)

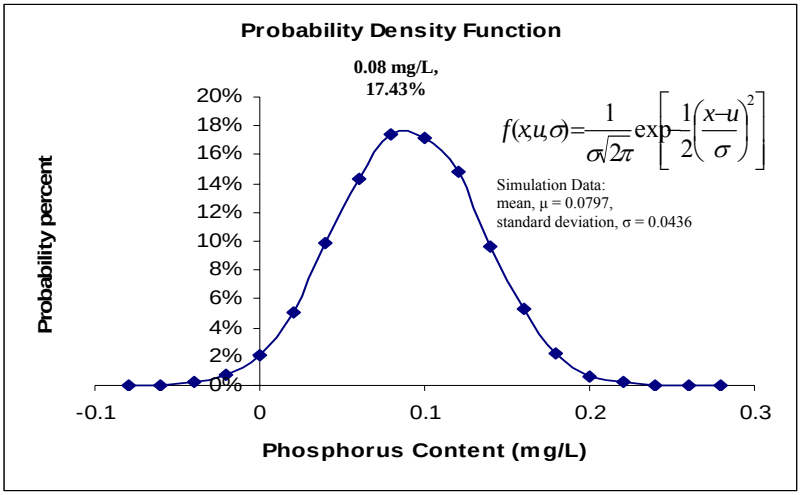

Figure 4.17: Monte Carlo simulation of phosphorus concentration (mg/l)

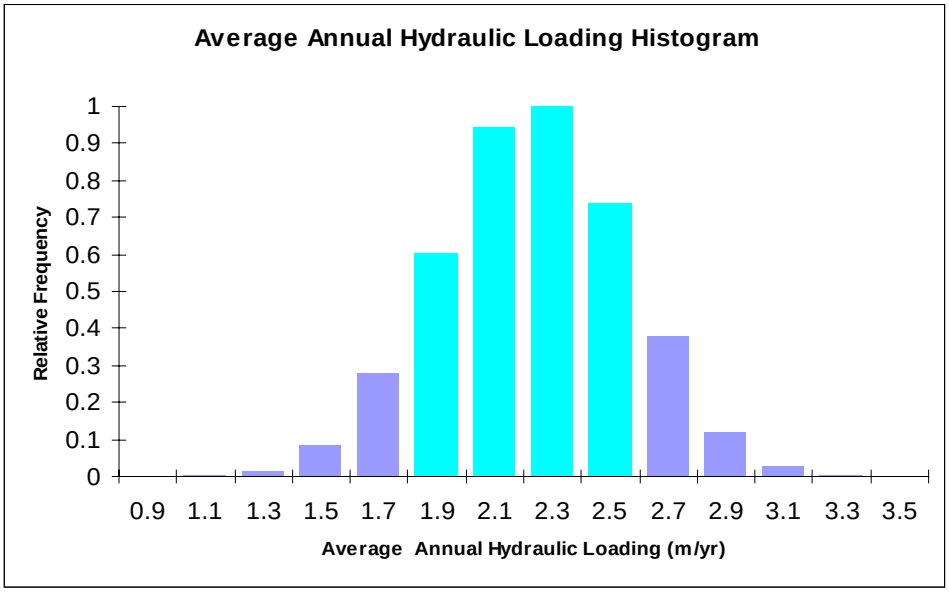

Figure 4.18: Normal distribution of hydraulic loading (m/yr)

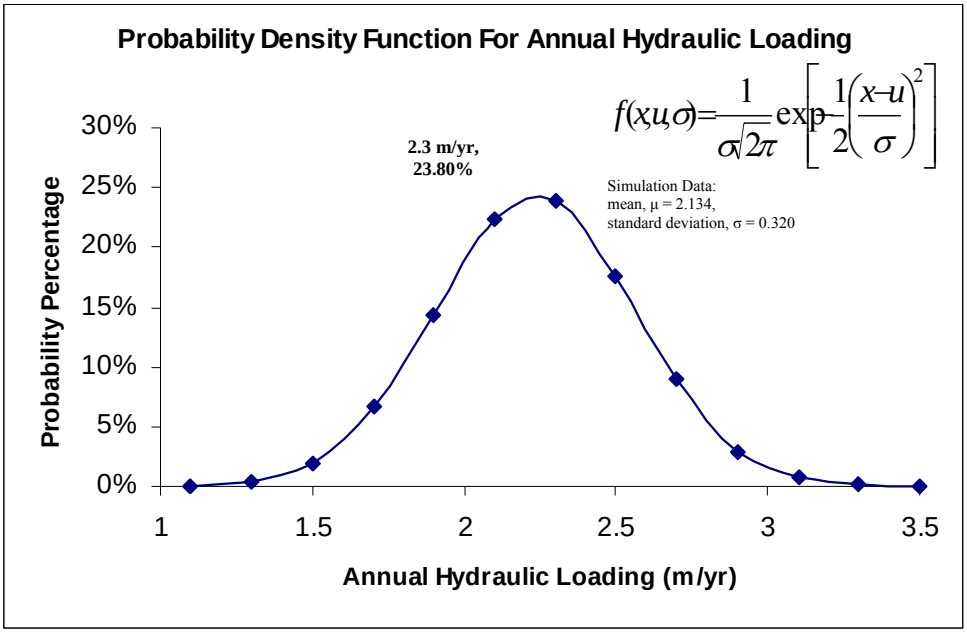

Figure 4.19 : Monte Carlo simulation of hydraulic loadings (m/yr)

Figure 4.16, showed the most likely range of phosphorus content obtained was 0.06 mg/l to 0.12 mg/l based on 4 highest histogram. The average phosphorus content was 0.0801 mg/l from Monte Carlo probability density function with probability percentage as many as 17.43% through normal distribution using phosphorus (mg/l) average simulation data of 0.0797 mg/l and standard deviation 0.0436.

Figure 4.18, the most likely range of annual hydraulic loading was 1.9 m/yr to 2.5 m/yr based on 4 highest histogram. The average annual hydraulic loading was 2.134 m/yr from Monte Carlo probability density function with probability percentage as many as 23.80% through normal distribution using hydraulic loading (m/yr) data simulation average of 2.134 m/yr and standard deviation 0.320.

To get the annual phosphorus loading, the two range and mean of phosphorus and hydraulic loading are combined through simple multiplication. The average phosphorus loadings obtained was 0.330 $g/m^2/yr$ (10.065 ton/yr), within the estimated range of 0.220 $g/m^2/yr$ to 0.578 $g/m^2/yr$ (6.710 ton/yr to 17.629 ton/yr).

CHAPTER 5

CONCLUSIONS AND RECOMMENDATIONS

5.1 Conclusions

The estimated range for phosphorus loading were from 0.1 g/m^2/yr to 3.71g/m^2/yr, as described by the fuzzy membership function. The most likely range occurred when the membership value in the membership function was 1. The boundaries of the membership function were 0.1 g/m^2/yr to 3.71 g/m^2/yr (3.09 ton/yr to 111.31 ton/yr) based on the input data. The core of the membership function were 0.26 g/m^2/yr to 0.81 g/m^2/yr (7.81 ton/yr to 24.28 ton/yr), which indicate the most likely range of occurring.

The performance of the IHACRES model in predicting the streamflow was measured based on the statistics obtain from the model simulation, which were the bias and R^2 value. The largest bias was -0.5546 mm/day and the smallest bias was -0.0076 mm/day. The bias value should be as close to zero as possible for optimal model performance. The highest R^2 value was 0.9925 and the lowest value was 0.9208. The R^2 value should be as close to one as possible. Both statistics indicated that the model was able to perform well.

The fuzzy membership function was developed to represent the uncertainty of the phosphorus loadings estimation. The range of minimum and maximum values for parameter of Vollenweider model could be obtained from the fuzzy membership function.

The average phosphorus content was 0.0801 mg/l from Monte Carlo probability density function with probability percentage of 17.43% through normal distribution. The average annual hydraulic loading was 2.134 m/yr from Monte Carlo probability density function with probability percentage of 23.80% through normal distribution.

There were two models used in this study, which were Vollenweider model and IHACRES model. All models were not perfect, but predictions or estimations could be made by using the models, which could later provide a better insight regarding to eutrophication related problems. Phosphorus loadings were expected to increase in the future from the activities observed in the catchment area. Therefore, proper management and mitigation were required to control the eutrophication either at the point sources or non-point sources.

5.2 Recommendations

Some suggestions and recommendations could be made for this study to improve the performance or the quality of the data and the results.

i) Site investigations could be done more often to increase the quantity of the data and samples. These data would be used in fuzzy membership function to

represent the actual condition throughout the catchment area. The representation would be more accurate when more data are collected.

ii) The stations for study could be added to increase the amount of data and set up at various points thoughout the study area. The locations and distribution of the stations should be arranged so that they represent the study area as a whole.

iii) Streamflow recording stations could be set up at the study area to obtain the actual streamflow of the study area. This will increase the quality of the data and improve the quality of the result generated.

iv) Study or research could be done in searching and obtaining computer softwares or programs that could generate histogram and fuzzy membership functions. This will help in saving time and increase the easiness to generate the histograms and membership functions and also to obtain the desired results.

REFERENCES

Debarry, P. A. (2004), "Watersheds Processes, Assessment, and Management.", New Jersey : John Wiley & Sons, Inc.

Dong, W. and Shah, H. C. (1987), "Vertex Method for Computing Functions of Fuzzy Variables." Fuzzy Sets and Systems, Vol. 24 65-78.

Evans, J. P. and Jakeman, A. J. (1998), "Development of a Simple, Catchment-Scale Rainfall-Evapotranspiration-Runoff model" Environment Modeling Software, Vol. 13, 385-393.

Faradilah Abd Rahman (2006), "Fuzzy Analysis for Vollenweider Phosphorus Loadings Model at Layang Reservoir Systems", Degree thesis, Universiti Teknologi Malaysia.

Galindo, J. Urrutia, A., Piattini, M. (2006), "Fuzzy Databases Modeling, Design and Implementation", Hershey : Idea Group Publishing.

Hammer, M. J. and McKichan, K. A. (1981), "Hydrology and Quality of Water Resources", New York : John Wiley & Sons, Inc.

Herschy, Reginald W. (1995), "Streamflow Measurement", 2nd edition, London : E & FN Spon.

Hong X.L. and Vincent C. Y. (1995), "Fuzzy Sets and Fuzzy Decision Making", CRC Press.

Jakeman, A. J. and Hornberger, G. M. (1993), "How Much Complexity is Warranted in a Rainfall-Runoff Model?" Water Resource Research, Vol. 29 2637-2649.

Johor Bahru Heath Department Report. (1996), “Laporan Kajian Kebersihan Sistem Bekalan Air Logi Sungai Layang”.

Linsley, Jr. R. K., Kohler, M. A. and Paulhus J. L. H. (1988), “Hydrology for Engineers”, UK : McGraw-Hill Inc.

McCuen, R. H. (2005), “Hydrologic Analysis and Design”, 3rd edition, New Jersey: Pearson Education, Inc.

Norliza Othman (2005), “Hydrologic Characterictics of Putrajaya Lake.” Degree Thesis, Universiti Teknologi Malaysia.

Ross, T. J. (2004), “Fuzzy Logic with Engineering Application” 2nd edition, England : John Wiley & Sons Ltd.

Schnoor, J. L. (1996), “Environmental Engineering : fate and transport of pollutants in water, air, and soil.”, New York : John Wiley & Sons, Inc.

Sek Liang Chai (1997), “Pengurusan Kawasan Tadahan: Anggaran Pembebanan Fosforus: Kajian Kes Reservoir Sungai Layang.” Degree Thesis, Universiti Teknologi Malaysia.

Supiah Shamsudin (1997), “Phosphorus Loadings Estimation and Eutrophication Status of Sungai Layang Reservoir Using Vollenweider Model.” Jurnal Kejuruteraan Awam. Jil. 10, Bil.2, pp. 32-43.

Thomann, R. V. and Mueller, J. A. (1987), “Principles of Surface Water Quality Modeling and Control.”, New York : Harper & Row, Publishers, Inc.

Viessman, W., Jr., Lewis, G. L., Knapp, J. W. (1989), “Introduction to Hydrology”, 3rd edition, Singapore : Harper & Row Publisher Inc.

Wurbs, R. A. and James, W. P. (2002), “Water Resouces Engineering.”, Upper Saddle River, NJ : Prentice Hall.

APPENDIX A

Photos taken during site visit

Figure A.1 : View of Layang river

Figure A.2 : Another view of Layang river

Figure A.3 : View of Layang river wetlands

Figure A.4 : View of Ban Foo River

Figure A.5 : View of Layang Reservoir

Figure A.6 : Another view of Layang Reservoir

Figure A.7 : Water sampling

APPENDIX B

Tools and equipments used

Figure B.1 : Water sampling using water sampler

Figure B.2 : Measuring velocity using current meter

Figure B.3 : DR4000 Spectrophotometer